

## [Supplementary material]

### **Materials in movement: gold and stone in process in the Upton Lovell G2a burial**

Rachel J. Crellin<sup>1,\*</sup>[ORCID: 0000-0002-8297-1083], Christina Tsoraki<sup>1</sup>[ORCID: 0000-0001-9282-0847], Christopher D. Standish<sup>2</sup>[ORCID: 0000-0002-9726-295X], Richard B. Pearce<sup>2</sup>, Huw Barton<sup>1</sup>[ORCID: 0000-0002-3720-5435], Sarah Morriss<sup>1</sup> & Oliver J.T. Harris<sup>1</sup>

<sup>1</sup> School of Archaeology and Ancient History, University of Leicester, UK

<sup>2</sup> School of Ocean and Earth Science, National Oceanography Centre Southampton, University of Southampton, UK

\* Author for correspondence ✉ rjc65@le.ac.uk

## **Contents**

OSM1: microwear analysis of grave goods from Upton Lovell G2a, Wiltshire (including Figures S1–S3)

OSM2: SEM-EDS analysis of traces on objects from Upton Lovell G2a (including Figures S4–S29)

OSM3: summary data tables (see supplementary Excel file).

Table S1. Concordance table detailing the terminology used by previous authors to describe the various grave goods from Upton Lovell.

Table S2. Summary data regarding the production and making of different sheet gold items discussed in research by Woodward and Hunter (2015) and associated papers.

## **OSM1: microwear analysis of grave goods from Upton Lovell G2a, Wiltshire**

### **Methodology**

The analysis of the Upton Lovell G2a objects draws upon a broader body of technological and microwear studies of ground stone assemblages with well-established methodologies (Adams 2002; Tsoraki 2008, 2012, 2021; Adams *et al.* 2009; Dubreuil *et al.* 2015). All stone, flint and copper-alloy tools were subjected to technological and microwear analysis combining low and high-power analysis (e.g. Adams *et al.* 2009; Dubreuil *et al.* 2015; van Gijn 2010; 2014). Low power analysis (up to  $\times 100$ ) was conducted with a stereomicroscope (Leica M80) with an external, oblique light source. High-power analysis was conducted with an incident light (metallographic) microscope (Leica DM1750M, at  $\times 100$  and  $\times 200$

magnification) and with a stereomicroscope with a coaxial illumination unit (Leica M80 LED5000 CXI, at magnifications up to  $\times 230$ ). Micrographs were taken with a Leica MC120HD digital camera and Z-stacks were created with the Helicon Focus software. Wear features recorded include grain edge rounding, levelling, grain extraction, the presence and distribution of striations and other linear features, micropolish features including morphology and development, microstriations, microfractures, and the presence of residues (Hamon 2008; Adams *et al.* 2009; Dubreuil *et al.* 2015; Hayes *et al.* 2018). The microwear patterns observed on the archaeological tools were interpreted in relation to the reference collection of experimentally used tools housed at the Laboratory for Material Culture Studies at Leiden University, as well as published data (e.g. Caricola *et al.* 2020; Hamon *et al.* 2020). The Leiden reference collection comprises tools used for the processing of a wide range of vegetal, mineral (e.g. flint, basalt, amphibolite, clay and hematite) and animal materials (see also van Gijn & Houkes 2006; Verbaas & van Gijn 2007; Li *et al.* 2018).

### **Microwear analysis: results**

#### *DZSWS:STHEAD.1f: copper-alloy awl (Figure S1)*

The copper-alloy awl, which survives almost complete, belongs to the group of single-pointed awls with tang (Group 2A/B chisel-ended tang; Woodward & Hunter 2015: 89); one end has a flat transverse section, while the pointed end has a circular section. The awl exhibits differential corrosion at the tang and at the pointed end with more corrosion present at the latter. Diagonal grinding/polishing striations from manufacture are visible on the flattened tang (Figure S1Aa), which also shows indentations and plastic deformation (folding) on the sides and on the damaged end (Figure S1Ab) possibly associated with hafting. The tip of the awl is flat and shows rounding and a U-shaped depression at the centre (Figure S1Ba & S1Bb), suggesting it was used prior to its deposition in the burial. The wear traces on the tip of the awl suggest use with compressive force against a material of medium hardness, and not use against a very soft material such as human flesh (cf. Woodward & Hunter 2015: 96).

We considered the use of this item as a chasing tool or tracer. According to Armbruster (2017), a tracer with a sharp cutting edge was used to create decoration on gold surfaces, particularly deep lines. The end of this particular awl is not sharp and differs from other awls that have a chisel end. Moreover, the U-shaped depression on the tip and the distribution of wear traces suggests that the whole flat tip came into contact with the worked material. We

therefore retain the term ‘awl’ which is a broader term that carries less functional connotations than tracer or chasing tool.

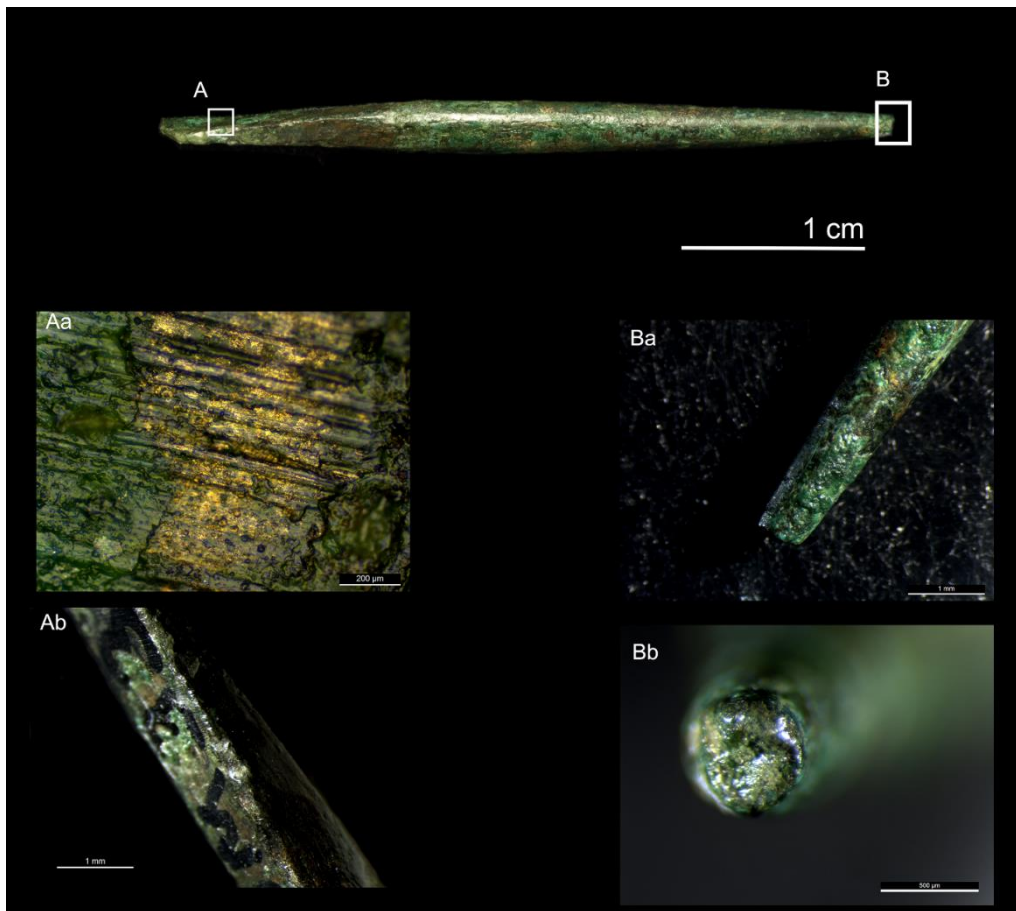


*Figure S1: Microwear traces on copper-alloy awl DZSWS:STHEAD.1f: Aa) grinding/polishing striations associated with the production stage; Ab) indentations and plastic deformation on the sides of the awl; Ba and Bb) rounding and a U-shaped depression at the centre of the flat tip (figure produced by C. Tsoraki; photographs courtesy of Wiltshire Museum, Devizes).*

*DZSWS:STHEAD.4a: broken battle axe (Figure S2A)*

DZSWS:STHEAD.4a is a battle axe, that was found broken in two pieces: one piece includes the cutting edge and part of the upper body of the battle axe (DZSWS:STHEAD.4a \_1) and a second piece forms the lower part of the body and retains part of the central perforation and the butt end (DZSWS:STHEAD.4a \_2) (see also Tsoraki *et al.* 2020). According to Roe’s typological scheme (1966) this battle axe is attributed to Stage III D or to the Intermediate form in her subsequent simplified scheme (Roe 1979). The battle axe has a slightly expanded cutting edge and a rounded/slightly angular shaped butt.

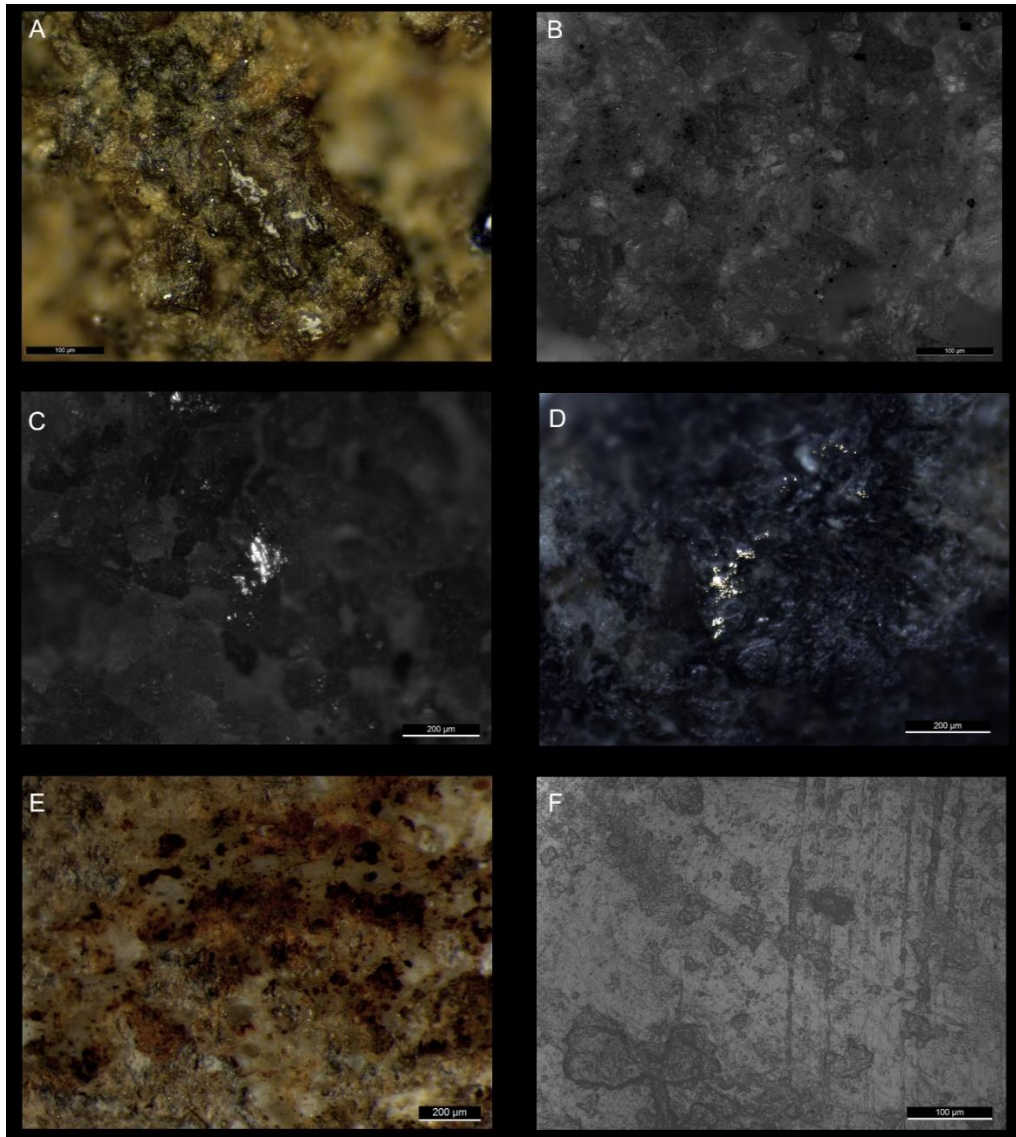


*Figure SI.2: Microwear traces on objects from the Upton Lovell G2a burial: A) micropolish with smooth texture, pitted appearance and a sinuous morphology on the cutting edge of battle axe DZSWS:STHEAD.4a ( $\times 200$  magnification); B) striated micropolish of flat to sinuous topography, smooth texture and pitted appearance on the surface of anvil DZSWS:STHEAD.3, ( $\times 200$  magnification); C) patch of highly reflective, striated micropolish on the surface of percussion tool DZSWS:STHEAD.6\_2, ( $\times 100$  magnification); D) gold-coloured residue traces forming a discontinuous streak on the surface of percussion tool DZSWS:STHEAD.6\_4; E) red-brown coloured residue and levelling of the surface topography on the surface abrading slab DZSWS:STHEAD.5 ( $\times 64$  magnification); F) micropolish of flat topography and rough texture accompanied by deep, parallel grooves and multi-directional striations on the surface of flint axe DZSWS:STHEAD.9 (figure produced by C. Tsoraki; photographs courtesy of Wiltshire Museum, Devizes).*

The battle axe is dark greenish grey in colour and is made from a medium-grained quartz dolerite, that derives from the Whin Sill in Northumberland in the northeast (Group XVIII) (Evens *et al.* 1962: 248, 1972: 257; Roe 1966: 245; but see Williams-Thorpe *et al.* 2003 for the identification of glacial erratics from the Whin Sill in southern Britain). Following the pecking of the battle axe with a hammerstone (pecking traces are more prominent on the margins and around the perforation), the axe was then ground and polished all over, although the surface was never polished to a high degree. The polishing was affected by contact with a hard mineral material as indicated by localised patches of a reflective micropolish with flat topography that develops on the higher elevations of the microtopography and is associated with fine micro-striations. Moreover, the battle axe is decorated with a wide, shallow double groove along its margins. The double groove has a polished interior and extends from the area near the cutting edge towards the lower part of the body and frames the perforation. The diameter of the perforation is 18mm and 20mm on either margin. The interior of the perforation is polished (with a directionality parallel to the long axis of the perforation) and its topography is characterised by the levelling of grains, occasional grain extraction and under high magnification a micropolish with a localised distribution that develops on the higher microtopography and is consistent with contact with a hard mineral material. The polishing obscures the concentric striations that resulted from the drilling process, which presumably entailed the use of a solid or hollow drill along with an abrasive material (e.g. sand) and a lubricant (e.g. water). While we have only a partial understanding of wear development in the interior of the perforation, no wear traces associated with hafting are visible on the preserved part of the perforation.

Different episodes of use have resulted in a worn-out cutting edge that exhibits heavy edge damage and intense rounding. Low-power observations include grain edge rounding accompanied with grain extraction from use in a percussive activity. Percussive traces extend across the cutting edge, while both expanded ends of the cutting edge have been flattened from localised secondary percussive use. At high magnification a reflective micropolish with localised distribution that follows the grain topography, has a smooth texture, pitted appearance, a sinuous morphology and in places is characterised by troughs and fine striations is observed on the cutting edge (Figure S2A), but not on the tips of the expanded ends. This type of micropolish and associated features are consistent with contact with a medium hard material (wood/bone), most likely bone. Polish development across the cutting edge, however, is limited and one of the reasons for this is the subsequent reuse of the battle

axe as a different form of percussion implement. Traces of this reuse are best seen on the flattened tips of the expanded ends that exhibit heavy edge damage.

Following the breakage of the battle axe in two pieces, the end of the upper body piece (where the perforation would have been originally) was intentionally re-shaped by pecking and grinding/low level polishing (post-manufacture modification). This form of modification may have been necessitated by the intention to transform this piece of the battle axe into a hammerstone. No attempt was made to re-shape and potentially remove the remaining part of the perforation from the lower part of the battle axe. Instead, the observed rounding seen on the higher aspects of the topography of the fractured edges around the perforation is consistent with weathering processes. Percussive traces of consistent appearance are present along the circumference of the butt end. The resulting pits show occasional rounding, but in places interrupt the ground/polished surface. While these traces could potentially relate to a subsequent reuse of the piece for percussive activities (i.e. as a hammer), based on the uniformity in their appearance (consistent depth, lack of flake removals and of sharp angular fractures, regular distribution across the circumference of the butt) it is also possible that they might relate to an attempt to reshape this area of the object.

Traces of a gold-coloured reflective residue that develop in a disrupted streak are visible on the cutting edge and on both margins, but it was not possible to conduct a compositional analysis of these traces with the SEM-EDS (see also section on SEM-EDS analysis).

*DZSWS.STHEAD.8: battle axe (Figure S3)*

STHEAD.8 is a complete battle axe, made from medium-grained igneous rock (dolerite) and is attributed to Stage III A in Roe's (1966) typological scheme. The battle axe is polished all over and has a slightly expanded cutting edge. Pecking traces resulting from the manufacturing process survive near the perforation on either margin; these were smoothed over, but irregularities remain. Longitudinal striations from grinding are present across the surface; they are parallel to long axis at the centre of the body and diagonal near the margin. At high magnifications, manufacturing traces include patches of reflective micropolish of flat topography consistent with stone against stone contact. The perforation is biconically-drilled and concentric striations have been mostly obliterated by subsequent polishing of the



*Figure S3: Microwear traces on battle axe DZSWS.STHEAD.8: A) flattening of the tip of the flared end on the cutting edge accompanied by percussive traces and grain edge rounding, (magnification at  $\times 10$ ); B) flattening of the tip of the flared end on the butt end accompanied by percussive traces (magnification at  $\times 10$ ) (figure produced by C. Tsoraki; photographs courtesy of Wiltshire Museum, Devizes).*

perforation interior. Observed edge removals along the rim of the perforation may be associated with the hafting of the battle axe. The cutting edge is blunt, and there is no evidence to suggest that the battle axe was resharpened prior to deposition. Wear traces on the cutting edge include percussive traces—irregular pits randomly distributed across the cutting edge and at the two flared ends. The centre of the cutting edge shows flattening and specs of a residue with reflective appearance are visible here. Similarly, the centre of the butt end exhibits a rhomb-shaped flattened area. Both margins also exhibit flattening on the tip of the flared ends on the cutting edge and the butt end; this is accompanied by light percussive traces (no angular step fractures are observed) and grain edge rounding (Figure S3A & S3B). A flat, striated micropolish consistent with contact with semi-hard mineral of metallic origin with transverse directionality is observed on one of the margins. Specs of a gold-coloured

residue of reflective appearance are visible at the flared end on the margin of the butt end. The distribution of the wear traces suggests the reuse of the battle axe for light percussive activities.

*DZSWS:STHEAD.2: grooved abrader (Figure 2 in main article)*

A complete grooved abrader that is made from a medium-grained sandstone (see also Woodward & Hunter 2015: appendix VI) and has a centrally located groove on one face. The shallow, straight groove has a U-shaped profile (though in places the groove has a slight V-shaped profile) and runs longitudinally across the broad face of the object. The groove measures  $62.58 \times 18.27$  mm and its depth is approximately 3.5mm. The interior of the groove has an uneven topography and is characterised by grain extraction, grain edge rounding and in places by coalescing grain crystals that show levelling on the higher elevations and rounding at their edges. Linear traces in the form of wide striations/grooves run longitudinally along the groove interior. At high magnifications a highly reflective, striated, micropolish of flat topography that forms patches or develops on individual grains and with directionality parallel to the long axis of the groove is observed along the length of the groove (Figure 2B). Corresponding wear patterns are obtained by contact with semi-hard mineral materials, including metal (e.g. Delgado-Raack 2008; Delgado-Raack & Risch 2008; Hamon *et al.* 2020). A green-coloured residue, possibly copper, was present inside the groove (Figure 2C). Occasionally, a smooth micropolish that has a sinuous topography and pitted appearance, and is accompanied by fine striations, develops on the higher elevations of individual grains occasionally penetrating the interstices; this is consistent with wood contact (Figure 2A). On the opposite face, handling traces (grain edge rounding, micropolish with sinuous topography and greasy appearance, and localised distribution on individual grains) are visible in the indentation created when a piece of the body and margin was detached. Prior to its placement in the burial, the tool was used for the processing of at least two materials using a linear abrading motion. The presence of microwear traces consistent with different contact materials suggests that while the grooved abrader was part of the metalworking toolkit, it did not have an exclusive metalworking function; it was also employed for the processing of other materials, in this case the smoothing of thin, wooden implements. It was previously suggested that grooved abraders may have been used in pairs during the processing of shafts (Woodward & Needham 2012: 120), but no wear traces consistent with this suggestion are observed on the dorsal surface of the tool.

*DZSWS:STHEAD.2a: polishing stone (burnisher/'touchstone') (Figure 4 in main article)*

Intact implement that is obovate in plan view and survives complete. The object is made from metamorphic slate and was previously thin-sectioned (Evens *et al.* 1962: 248). Microwear analysis shows traces of manufacture and use on the surface of the object and suggests a clear interest in the creation of smoothed and polished surfaces prior to use. Except for Margin B, part of which retains the natural weathered surface, all other surfaces of the pebble have been intentionally modified by abrasion as suggested by the presence of closely distributed striations and the flattening of the margins and ends. The broad faces are slightly convex. At high magnifications, connecting patches of reflective micropolish of flat to sinuous topography develop on the higher elevations of the microtopography occasionally penetrating the interstices; wide striations and deeper grooves of different lengths run mainly parallel/diagonal to the long axis of the tool, but finer striations of transverse/diagonal directionality are also visible (Figure 4A & 4B). Multiple streaks of reflective, gold-coloured residue are visible both on the broad surfaces and on the narrow margins. Pronounced residues that form a streak are present at the junction of broad face B and the curved margin (Figure 4C); the streak has fine striations with longitudinal directionality suggesting a longitudinal abrasive motion. The gold-coloured streaks have transverse and longitudinal directionality suggesting that that the implement was held in different ways when it came into contact with gold materials.

The microwear patterns are consistent with the use of the object in an abrasive motion which may include the use of the object as a touchstone (see Boutoille 2019). Touchstones tend to be made of black-coloured and fine-grained rocks such as tuffs, cherts and siltstones (Moore & Oddy 1985). In the case of the Upton Lovell G2a example, while it remains a possibility, the presence of streaks alone are not enough to support the interpretation of the object as a touchstone. Instead, the location of the gold residues on both broad surfaces and on narrow edges and ridges along with the intentional shaping of the narrow sides of the implement suggest a function associated with the shaping/finishing (polishing) of small-sized/narrow gold surfaces.

*DZSWS:STHEAD.3: percussion tool (anvil) (Figure S2B)*

An intact implement that is circular in plan view, has faceted edges and is made from quartzite. The original nodule was a cobble. The broad faces of the implement are flat and slightly curving towards the edges. They have been intentionally shaped by grinding and

polishing. The topography of the microrelief has a sinuous appearance and the grain crystals show edge rounding and in places levelling.

Impact fractures in the form of indentations and shallow pits of different shapes cut through the polished surface on both broad faces. On Face B a main percussion zone is located at the centre of the use-face, but diffuse impact fractures are visible across the surface and towards the edges of the tool. No angular step fractures and deep grain removals are present. At high magnifications, microfractures are visible on the higher elevations of the grain crystals and localised patches of reflective micropolish are observed across the surface. A striated micropolish of flat to sinuous topography, smooth texture and pitted appearance develops in patches that affect mostly the higher elevations of the microtopography suggesting contact with a semi-hard material of mineral origin (cf. Hamon *et al.* 2020) (Figure S2B). Metal residue traces forming an interrupted streak are visible on both faces. The microwear traces are consistent with the use of the implement for fine percussion activities of semi-hard mineral materials. This together with the intentionally polished surface would be consistent with the use of the tool as a lower stable tool and more specifically as an anvil for metalworking activities during the shaping and finishing of metal sheets (cf. Boutoille 2019).

*DZSWS:STHEAD.6\_1: percussion tool (anvil)*

NB: The museum accession numbers DZSWS:STHEAD.6 and DZSWS:STHEAD.4 refer to a group of five and four objects respectively. During the microwear analysis an additional number (e.g., DZSWS:STHEAD.6\_1, DZSWS:STHEAD.4\_2, etc) was added to the original museum accession number in order to create an individual ID record for each object within each group.

A complete, red-coloured quartzite cobble that is ovate in plan view and plano-convex in section. One broad surface is flattened with slightly convex edges and is intentionally shaped by polishing. On this face the topography of the microrelief has a sinuous appearance and the grain crystals show edge rounding and in places levelling. Impact fractures (pits) cut through the polished surface and display smoothing and rounding suggesting a concomitant abrasive and percussive action. At high magnifications, microfractures are visible on individual grains, along with localised patches of reflective, rough and pitted micropolish that develop on the higher elevations of the microtopography and are distributed across the surface. Occasional linear features include fine striations. Metal residue traces forming an interrupted streak are visible on this face. The opposite convex face has a more irregular topography. The wear

traces are consistent with the use of the tool as a lower stable tool (anvil) for metalworking activities during the shaping and finishing of metal sheets.

*DZSWS:STHEAD.6\_2: percussion tool (Figure S2C)*

A complete, sub-square quartzite cobble that shows wear traces on both broad surfaces and on three narrow ends (five use-faces in total). One of the broad use-faces shows levelling of grain crystals, and has been intentionally shaped by abrasion, but it is not polished to the same degree as DZSWS:STHEAD.6\_1. In places, patches of smooth, flat micropolish are visible, but the micropolish is not well developed. Further microwear traces include localised patches of a highly reflective, striated micropolish that forms interrupted bands with oblique directionality (Figure S2C). Three narrow ends were used for pounding and exhibit shallow impact fractures and grain edge rounding. At high magnifications, one of the narrow ends displays microfractures accompanied by localised patches of flat, smooth, reflective micropolish. Possible light brown coloured residue is also visible on this surface. The microwear traces are consistent with the use of the broad surface of the tool for hammering and smoothing metal surfaces, while the ends for pounding activities.

*DZSWS:STHEAD.6\_3: percussion tool (Figure 6 in main article)*

A complete implement made from Group I rock, a type of greenstone whose source is located in Cornwall and possibly in the Mount's Bay area near Penzance (Evens *et al.* 1962: 211 & 248, 1972). It is broadly parallelepiped in plan view and dark green in colour. One of the narrow ends is flat and curving towards the edges of the tool (as seen in Figure 6). It may represent a reworked battle-axe that has been reshaped and polished on all surfaces.

The surface of the object was intentionally polished and at high magnifications patches of micropolish with flat topography and smooth texture, or in places a combination of smooth/rough-textured micropolish, develop on the higher elevations of the microtopography (Figure 6A). This well-developed micropolish is consistent with hard mineral contact and more specifically stone on stone contact that has resulted from the intentional polishing of the tool surface. The polished surface is interrupted by impact fractures (pits of irregular sizes), while the fractured grain crystals do not display edge rounding suggesting that the percussion was the last action. At high magnifications, microfractures of angular morphology are associated with a highly reflective, flat, striated micropolish of oblique directionality that develops in elongated discontinuous streaks and affects the higher microtopography (Figure 6B). In places, this type of micropolish is associated with gold-coloured reflective residue

traces (Figure 6C). One of the narrow ends also exhibits brown-coloured residues trapped inside pits. The intentionally polished surface, the combination of impact fractures and micropolish consistent with contact with a semi-hard mineral material suggest the use of the implement for percussive actions associated with metalworking.

*DZSWS:STHEAD.6\_4: percussion tool (Figure S2D)*

This implement bears many similarities with DZSWS:STHEAD.6\_3 in terms of morphology (broadly parallelepiped in shape, flattened use-faces curving towards the edges of the tool) and wear traces. Similar to the DZSWS:STHEAD.6\_3 it is also made from a greenstone, but this example is attributed to Group IIIa, also of Cornish origin (Evens *et al.* 1962: 248). The object is complete and is shaped by polishing, but one of the surfaces was only partially ground and polished. Microwear traces, though not well developed, include a highly reflective, striated micropolish, that forms a band, percussive traces and gold-coloured residue traces that form a discontinuous streak (Figure S2D). Observed wear patterns suggest that the implement was used in metalworking activities as a percussive implement.

*DZSWS:STHEAD.6\_5: percussion tool*

Complete quartzite cobble that has dark red/brown coloured residues on different surfaces. The surfaces, that are not ground/polished, have fractured grain crystals that exhibit angular step fractures. Occasionally the grain crystals exhibit edge rounding. The implement was used for percussion.

*DZSWS:STHEAD.5: abrading slab (Figure S2E)*

A slab made from a well-cemented sandstone that is triangular in plan view and almost square in section. It is missing one end. The surface topography is irregular, and all faces show localised smoothing, grain edge rounding and some levelling. Red-brown coloured staining (possibly ochre/hematite) is found in association with the levelled areas and is present on different surfaces of the tool (Figure S2E). The microwear traces are consistent with the use of the tool for longitudinal abrasive actions as a lower stable tool.

*DZSWS:STHEAD.12: elongated pounding tool/pestle*

Elongated quartzite cobble that is light brown in colour. Light pounding traces are visible on the body and on one end. Wear traces include grain extraction, impact fractures which in places take the form of angular step fractures, and grain edge rounding. These wear traces are accompanied by possible metal residues.

*DZSWS:STHEAD.9: flint axe (Figure S2F)*

A complete flint axe that is patinated. The cutting edge and the body is polished and traces of the initial shaping of the axe in the form of flake removals are visible on both faces. The negatives of the removals were ground down but not completely erased. Microwear traces associated with the manufacture of the axe include linear features such as deep, parallel grooves and multi-directional striations of varied lengths, reflective micropolish of flat topography and rough texture that develops in patches (Figure S2F). The edges of the grooves and the striations show rounding and in places a rough micropolish, with sinuous topography that affects the higher microtopography, the intermediate area and occasionally the lower microtopography suggest contact with a soft material, possibly hide. The axe was resharpened as shown by a series of fine parallel striations with transverse directionality that cut through the wider grooves near the cutting edge. Part of the cutting edge has unifacial flake removals and at high magnifications a band of rough, micropolish with pitted appearance and sinuous topography develops across the cutting edge and is accompanied by microfractures and edge removals. In places, the micropolish has striations parallel to the cutting edge. The wear patterns are consistent with the use of the axe for woodworking. Gold-coloured residue traces that form a discontinuous streak are present at the centre of the cutting edge with a distribution from the cutting edge towards the body of the axe. Further residues with a metallic appearance are present on the cutting edge towards the margin of the flint axe.

*DZSWS:STHEAD.9a: flint axe*

A flint axe that survives complete. The surface is patinated and in places it has powdery texture associated with recortication. The cutting edge is flaked and the body is partially polished.

*DZSWS:STHEAD.9b: flint axe*

A flint axe that survives complete. The whole surface is polished and patinated and in places the polished surface exhibits light pitting and has powdery texture associated with recortication. A grey cherty inclusion is visible on Face A. The surface exhibits manufacturing wear traces that include longitudinal striations and at high magnifications wide grooves and patches of micropolish with flat topography that have resulted from grinding/polishing actions employing hard mineral (stone) and abrasive materials. Prior to polishing the surface was flaked to shape and the ridges of the flake removals show rounding. Wear traces on the cutting edge are concentrated on one end and include light chipping and mostly small bifacial and unifacial edge removals and some edge rounding. The other end has a single bifacial removal. Following the original manufacture and polishing the axe went through different episodes of modification and flakes were removed from the margin and the butt area. Moreover, an area on one of the margins shows crushing and multiple flake removals with hinge fractures are visible. These are similar in appearance with the wear traces observed on flint axe DZSWS:STHEAD.10 and would suggest that both implements were reused in crushing actions.

*DZSWS:STHEAD.10: flint axe*

Broken flint axe that has a heavily patinated surface. The original ground and polished surface was removed by subsequent flaking and survives only in places on the body and margin. The original cutting edge has been completely destroyed from reuse in a percussive activity employing a crushing motion. The surviving edge exhibits multiple flake removals and hinge fractures that are accompanied by edge rounding. Residue traces of slightly metallic appearance and of black/dark red colour (possibly hematite/ochre) are present along the edge. At high magnifications, the distribution of the residue traces is closely associated with patches of reflective micropolish, with sinuous topography and rough texture that is associated with oblique striations develops on the higher microtopography. This type of micropolish is consistent with contact with semi-hard mineral material. The opposite end also has flake removals and hinge fractures. The wear patterns and the mineral residues suggest the reuse of the implement for the crushing of minerals and most likely hematite.

#### *DZSWS:STHEAD.4: flint nodule cups*

The interior of cup DZSWS:STHEAD.4\_1 exhibits localised smoothing and is accompanied by black and dark brown residues.

The interior of cup DZSWS:STHEAD.4\_2 exhibits yellow/orange-colour staining accompanied by smoothing of grains and grain edge rounding. On the exterior surface there are flake removals on a protruding area at the bottom of the cup.

The interior of cup DZSWS:STHEAD.4\_3 exhibits grain edge rounding and brown orange staining. Intense rounding and polish is also observed on the exterior surface.

Cup DZSWS:STHEAD.4\_4 is the smallest cup. It has a centrally located hole which appears very regular, but no drilling traces are visible and seems natural. The interior of the cup shows grain edge rounding and smoothing.

### **OSM2: SEM-EDS analysis of traces on objects from Upton Lovell G2a**

#### **Methods**

Compositional analysis of the majority of possible metal traces, identified first with a stereomicroscope (Leica M80) and an incident light (metallographic) microscope (Leica DM1750M), were analysed non-destructively at the School of Ocean and Earth Sciences, University of Southampton, using a Carl Zeiss Leo 1450VP scanning electron microscope (SEM) coupled to an Oxford Instruments X-Act 10mm<sup>2</sup> area SEM-Energy Dispersive Spectrometer (EDS) and utilising the AZtec Energy software system. Traces on two objects, DZSWS:STHEAD.4a\_1 and DZSWS:STHEAD.9, were analysed at the School of Archaeology and Ancient History, University of Leicester, using a Carl Zeiss EVO25 SEM coupled to a Bruker XFlash 6/60 EDS. Characterisation of the background composition, i.e. that of the object itself, was performed prior to analysis of each trace. Elements present in the background analysis were then discounted when characterising the composition of the traces due to the likelihood that they relate to the bulk composition of the object rather than the trace itself. Concentrations of remaining elements were normalised to 100% for interpretation. A series of three custom-made gold-alloy reference materials from Micro-Analysis Consultants Ltd. were analysed as a demonstration of accuracy and precision: MAC1 (59.4% Au, 29.8% Ag, 9.1% Cu, 2.0% Sn), MAC2 (74.7% Au, 19.2% Ag, 5.1% Cu, 1.0% Sn) and MAC3 (93.9% Au, 4.6% Ag, 1.0% Cu, 0.5% Sn). Accuracy and external reproducibility (two standard deviations (SD) of the mean) are  $\leq \pm 5\%$  for elements with certified concentrations are  $> 5\%$ ,  $< \pm 20\%$  for elements with certified concentrations between

2% and 5%, and  $\leq\pm 50\%$  for elements with certified concentrations between 1% and 2%. Due to size restrictions of the SEM sample chamber housed at the University of Southampton, and the fixed position of its secondary electron detector, it was not possible to examine every artefact or every face of every artefact. This means not all traces, identified with the metallographic microscope could be analysed. In particular, the polished percussion tool DZSWS:STHEAD.6\_3 was not investigated due to size/shape restrictions. Furthermore, the cutting-edge portion of the battle axe DZSWS:STHEAD.4a\_1 was only partially analysed due to time constraints, and there are further possible residue traces present that were only identified with the metallographic microscope.

### Sampling locations and results

Two locations were analysed on the copper-alloy awl DZSWS:STHEAD.1f (Figure S4), where possible traces had been identified following visual inspection: two analyses at location 1, one analysis at location 2. No traces of metalworking were identified, with all analyses consistent with the copper alloy composition of the object itself (i.e. Cu and Sn), see OSM 3 (Excel file).



*Figure S4. DZSWS:STHEAD.1f sample locations (figure produced by C. Tsoraki; photographs courtesy of Wiltshire Museum, Devizes).*

Three analyses were performed on possible traces at one location on the grooved abraded DZSWS:STHEAD.2 (Figure S5). Traces were either Cu-alloys (one analysis; Figure S6), or Pb-based (two analyses).



Figure S5. DZSWS:STHEAD.2 sample location (figure produced by C. Tsoraki, photographs; courtesy of Wiltshire Museum, Devizes).

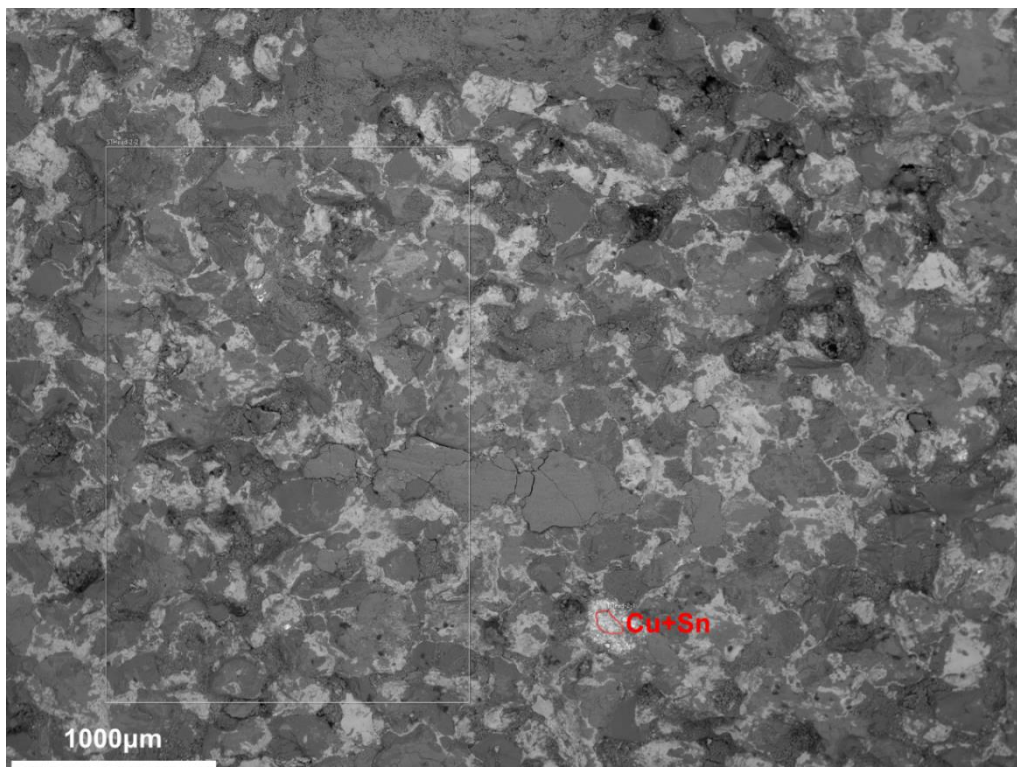


Figure S6. BSE image of DZSWS:STHEAD.2 showing Cu-alloy trace, with the analysed area defined by a red line. The rectangular region is the area where the background signal was measured (figure produced by C. Standish and R. Pearce).

Traces located at seven locations on the polishing tool DZSWS:STHEAD.2a were analysed; four on Face B (Figure S7: note location 1, not shown on the image, is where the background measurement was taken) and three on Face A (Figure S8). Back Scattered Electron Detector (BSE) images of all traces are shown in Figures S9–15. On Face A, location 8 contains traces of both Cu- and Au-alloys. The proximity of both traces, distinguishable in the SEM image (e.g. Figure S15), makes it impossible to quantify the composition of the Au trace and accounts for the high variability. This is a similar case for location 7 (Figure S14), which shows both Cu and Au traces. Location 6, (Figure S13) on Face A recorded a Pb-based reading. On Face B, 4 Au-alloy traces were characterised: on location 2 (Figure S9), a trace with a mean composition of  $85.7\% \pm 2.9\%$  Au,  $12.4\% \pm 2.6\%$  Ag and  $1.9\% \pm 0.3\%$  Cu (uncertainties are two SD of the mean) was identified, whilst on location 3 (Figure S10) a trace with a mean composition of  $85.0\% \pm 1.0\%$  Au,  $13.3\% \pm 1.0\%$  Ag and  $1.72\% \pm 0.01\%$  Cu was identified. Traces at locations 2 and 3 correspond to the area previously analysed by Shell (2000). On location 4 (Figure S11), a trace with a mean composition of  $92.8\% \pm 2.5\%$  Au,  $4.8\% \pm 2.4\%$  Ag and  $2.4\% \pm 0.1\%$  Cu was recorded; and on location 5 (Figure S12) a trace with a mean composition of  $92.6\% \pm 1.4\%$  Au,  $4.9\% \pm 0.4\%$  Ag and  $2.5\% \pm 1.1\%$  Cu was recorded.



*Figure S7. DZSWS:STHEAD.2a Face B sample locations (figure produced by C. Tsoraki; photographs courtesy of Wiltshire Museum, Devizes).*



Figure S8. DZSWS:STHEAD.2a Face A sample locations (figure produced by C. Tsoraki; photographs courtesy of Wiltshire Museum, Devizes).

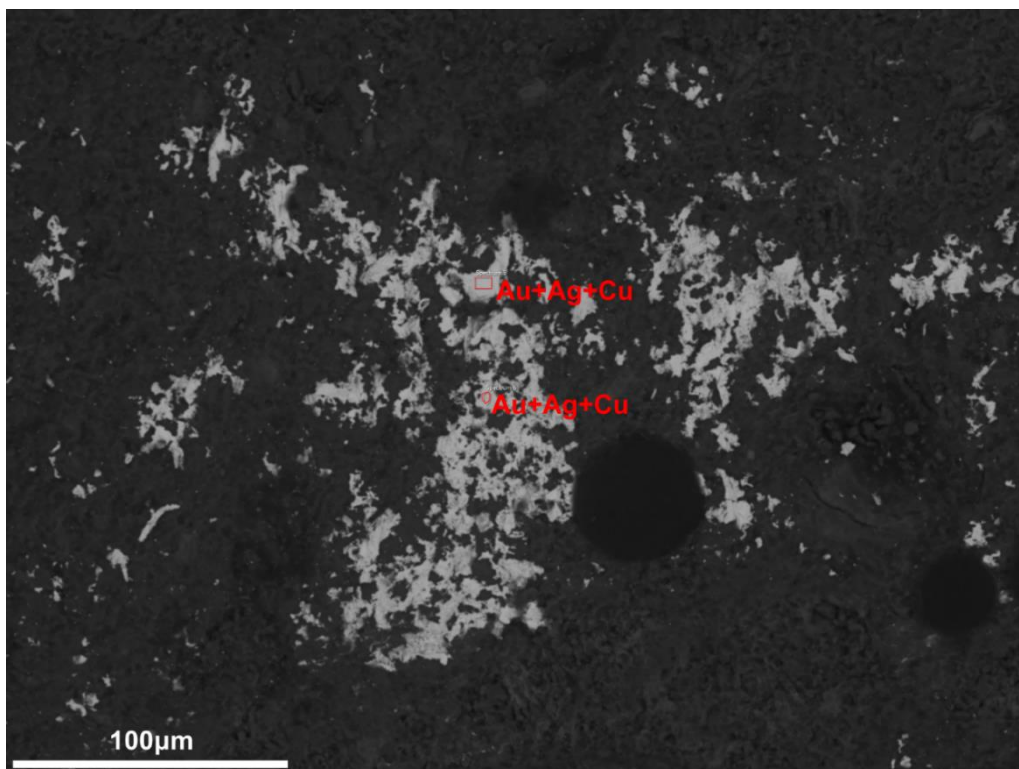
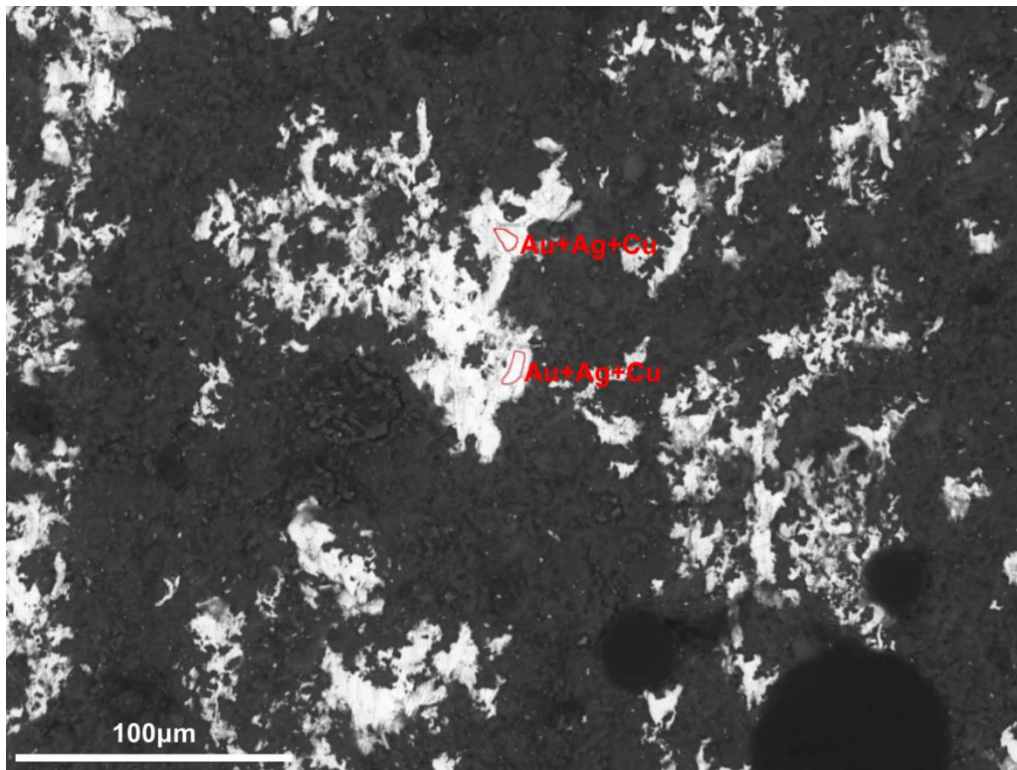
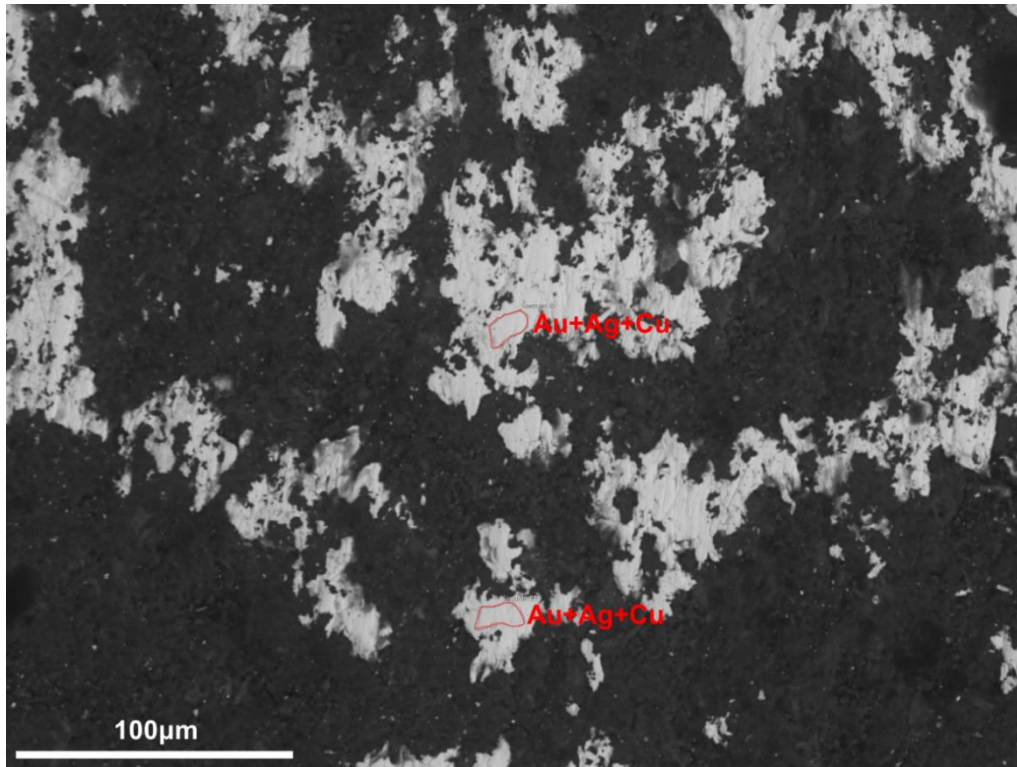


Figure S9. BSE image showing gold-alloy trace (brighter regions) within location 2 on DZSWS:STHEAD.2a. The areas analysed are marked in red (figure produced by C. Standish and R. Pearce).



*Figure S10. BSE image showing gold-alloy trace (brighter regions) within location 3 on DZSWS:STHEAD.2a. The areas analysed are marked in red (figure produced by C. Standish and R. Pearce).*



*Figure S11. BSE image showing gold-alloy trace (brighter regions) within location 4 on DZSWS:STHEAD.2a. The areas analysed are marked in red (figure produced by C. Standish and R. Pearce).*

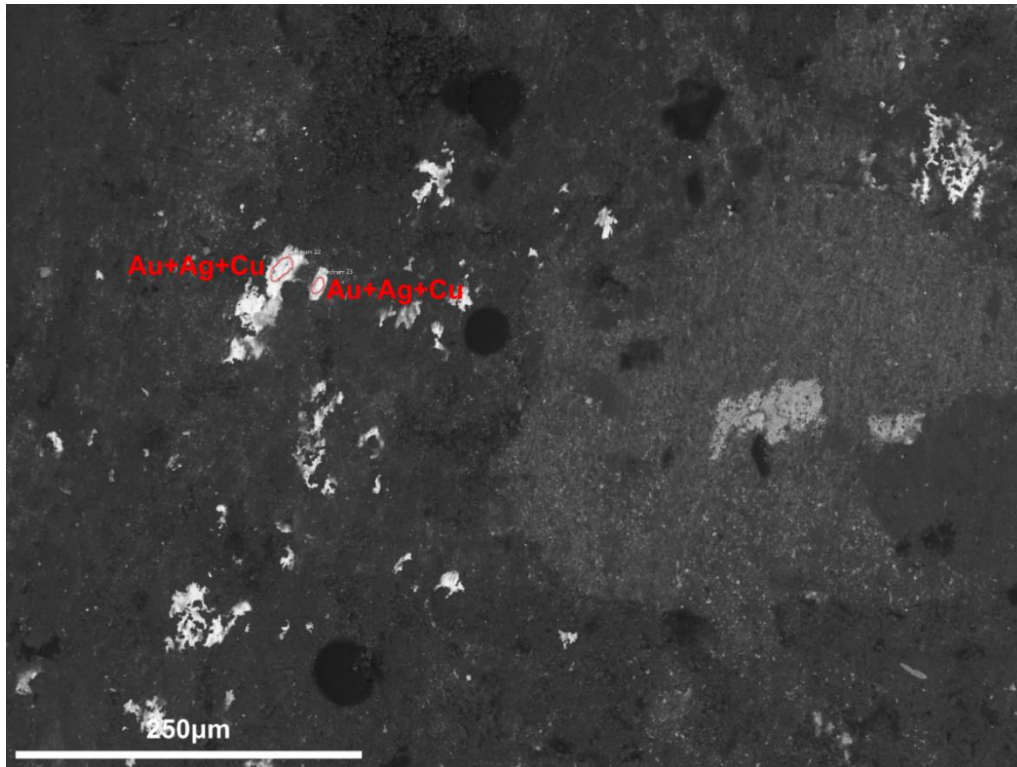


*Figure S12. BSE image showing gold-alloy trace (brighter regions) within location 5 on DZSWS:STHEAD.2a. The areas analysed are marked in red (figure produced by C. Standish and R. Pearce).*

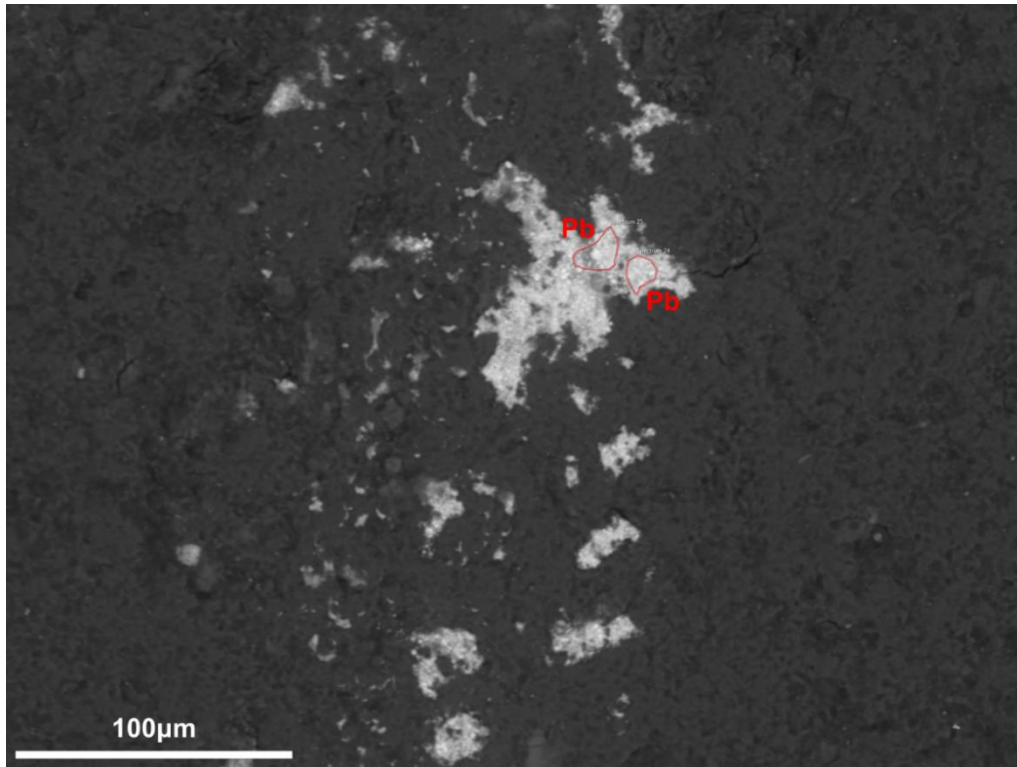


*Figure S13. BSE image showing lead trace (brighter regions) within location 6 on DZSWS:STHEAD.2a. The areas analysed are marked in red (figure produced by C. Standish and R. Pearce).*

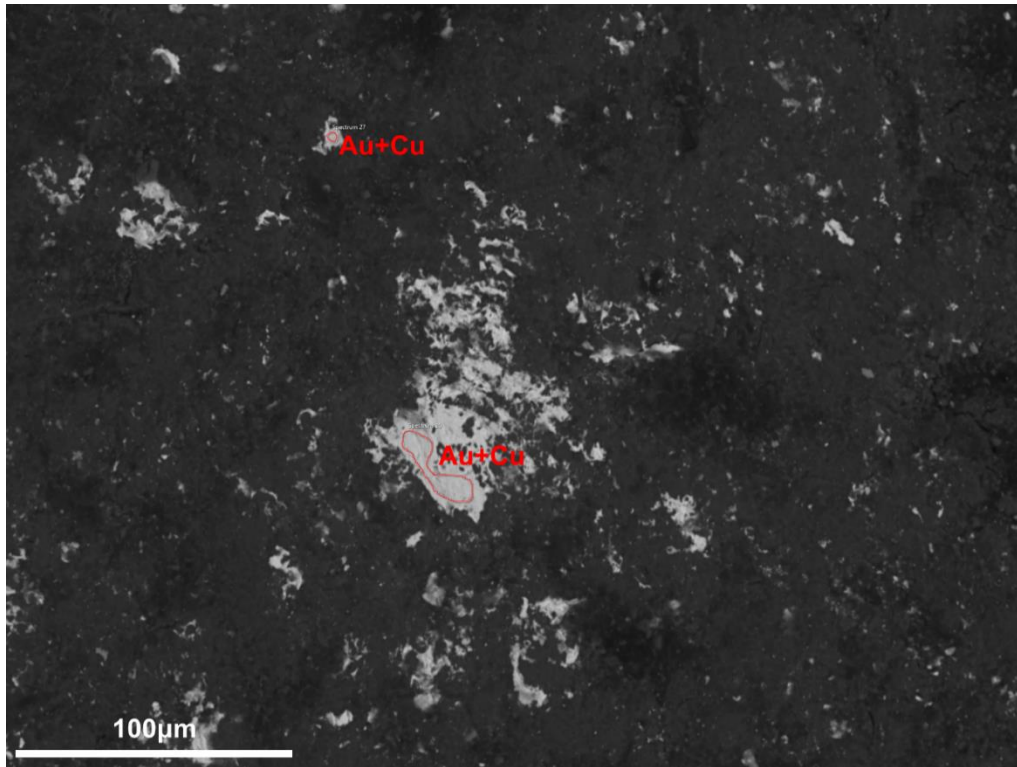


*Figure S14. BSE image showing gold-alloy trace (brighter regions) within location 7 on DZSWS:STHEAD.2a. The areas analysed are marked in red (figure produced by C. Standish and R. Pearce).*

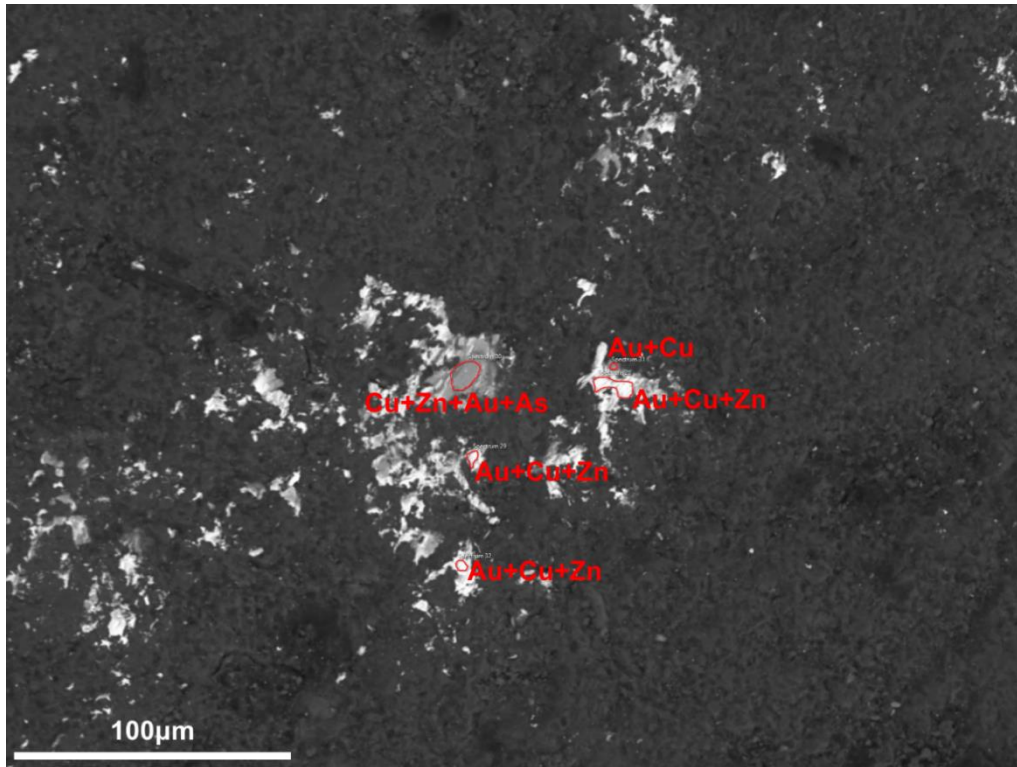


*Figure S15. BSE image showing metal trace within location 8 on DZSWS:STHEAD.2a. The areas analysed are marked in red. Gold-alloy traces are visible as brighter regions relative to the slightly duller copper-alloy traces (figure produced by C. Standish and R. Pearce).*

Two locations were investigated on the anvil DZSWS:STHEAD.3. Au-alloy traces were recorded at location 2 on Face A (Figure S16), with a mean composition of  $80.5\% \pm 3.0\%$  Au,  $12.1\% \pm 2.0\%$  Ag and  $7.4\% \pm 1.1\%$  Cu. A Pb-based reading was also recorded at this location, as well as at location1, Face B (Figure S17). Figure S18 shows a BSE image of the traces analysed at location 2.



*Figure S16. DZSWS:STHEAD.3 face A sample location (figure produced by C. Tsoraki; photograph courtesy of Wiltshire Museum, Devizes).*



*Figure S17. DZSWS:STHEAD.3 Face B sample location (figure produced by C. Tsoraki; photograph courtesy of Wiltshire Museum, Devizes).*

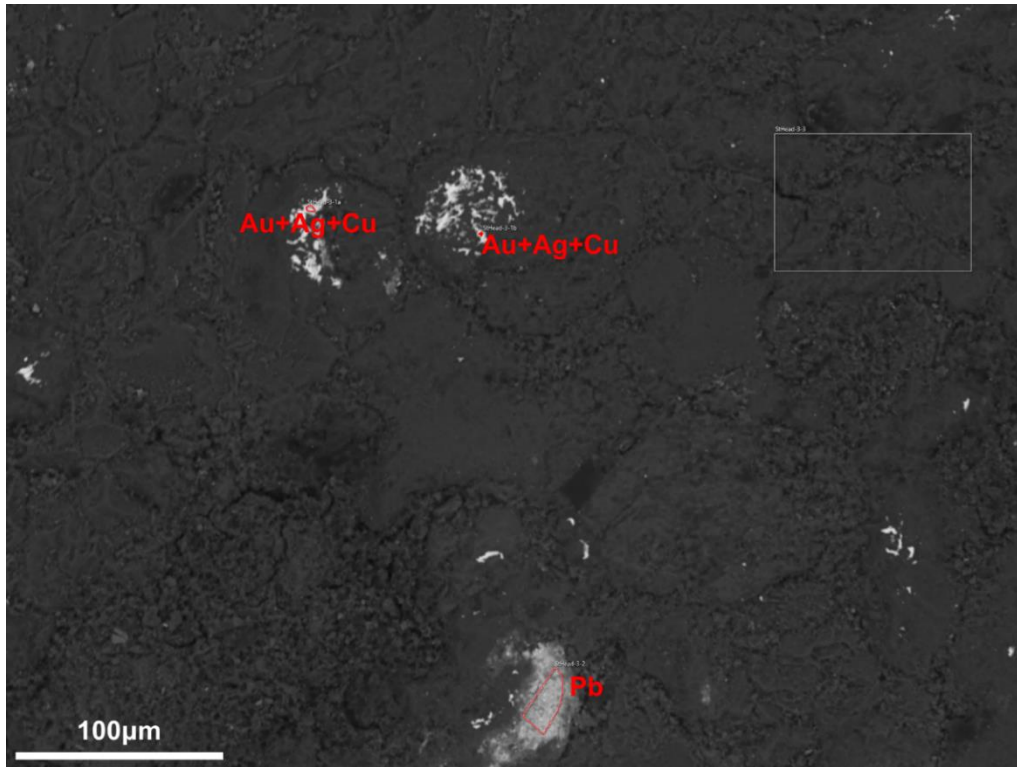


*Figure S18. BSE image showing metal traces analysed at location 2 on DZSWS:STHEAD.3. The areas analysed are marked in red, with the rectangular region being where the background signal being measured (figure produced by C. Standish and R. Pearce).*

Three analyses were performed on a trace located on the cutting edge of battle axe DZSWS:STHEAD.4a\_1 (Figure S19). They returned compositions indicating a Cu-Zn alloy (Cu ranging from  $72.9\% \pm 6.5\%$  to  $32.0\% \pm 2.5\%$  and Zn ranging from  $62.4\% \pm 5.0\%$  to  $24.9\% \pm 1.3\%$ ), along with minor quantities of Sn, Ag, Al, Fe and Sb (Figure S20). Further possible residue traces were also identified with the metallographic microscope but could not be further analysed due to time constraints.



*Figure S19. DZSWS:STHEAD.4a\_1 sample location (figure produced by C. Tsoraki; photographs courtesy of Wiltshire Museum, Devizes).*

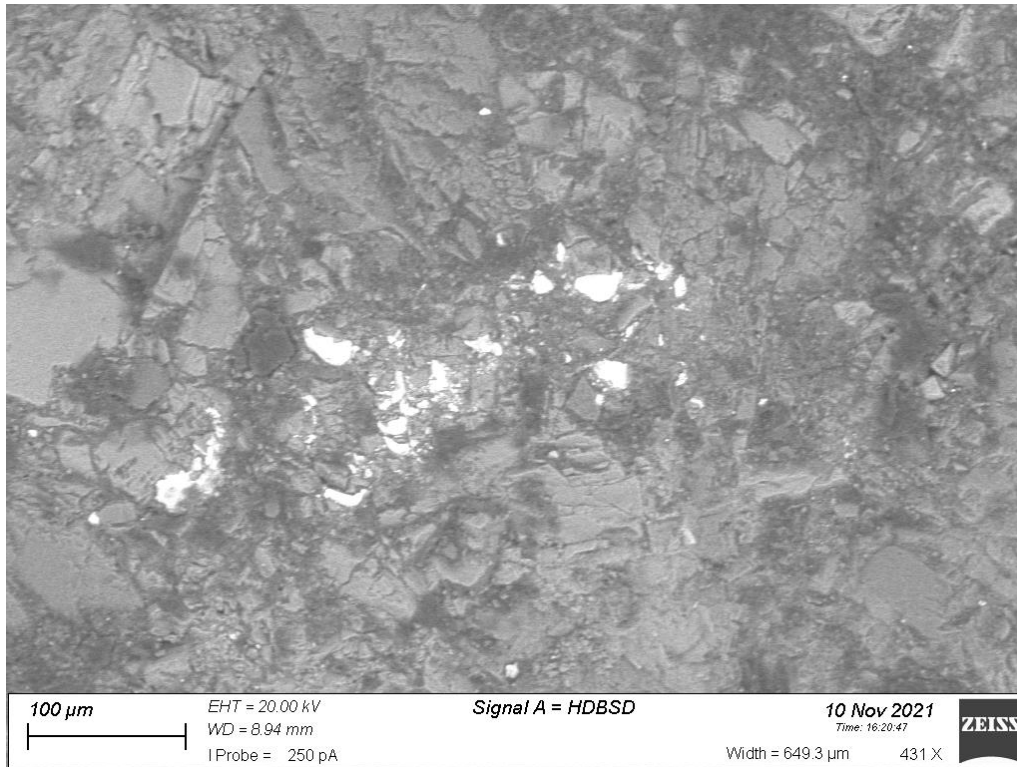


*Figure S20. BSE image of copper-zinc alloy trace (brighter regions) on DZSWS:STHEAD.4a\_1 (figure produced by S. Morriss and C. Standish).*

A trace within the perforation of the butt-end of battle axe DZSWS:STHEAD.4a\_2 was analysed (Figure S21). It returned a composition of  $84.1\% \pm 1.5\%$  Fe,  $15.3\% \pm 1.2\%$  Cr, and  $0.5\% \pm 0.3\%$  Mn (Figure S22).

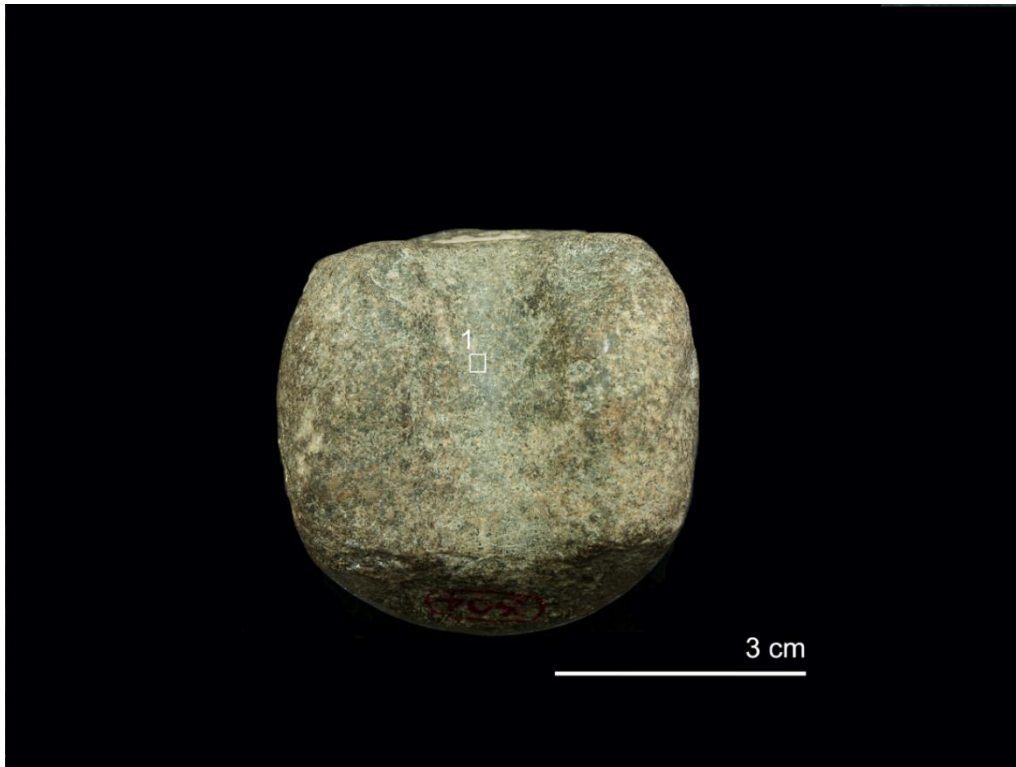


*Figure S21. DZSWS:STHEAD.4a\_2 sample location (figure produced by C. Tsoraki; photograph courtesy of Wiltshire Museum, Devizes).*

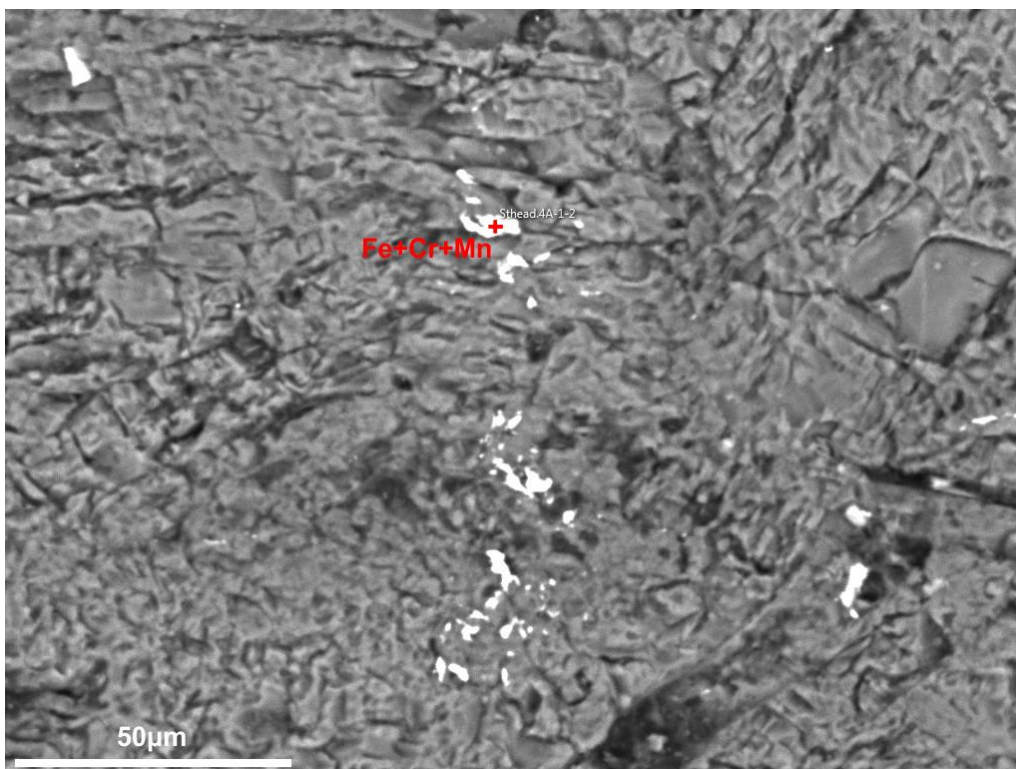


*Figure S22. BSE image of Fe-Cr-Mn trace, and one of the points analysed (red cross), on DZSWS:STHEAD.4a\_2 (figure produced by C. Standish and R. Pearce).*

A trace on anvil DZSWS:STHEAD.6\_1 was analysed (Figure S23). It recorded an Au-alloy with a mean composition of  $97.6\% \pm 0.7\%$  Au,  $0.7\% \pm 0.3\%$  Ag, and  $1.7\% \pm 1.0\%$  Cu (Figure S24). Other traces of Pb and Cu+Sn were also noted, but not quantified. A trace on percussive tool DZSWS:STHEAD.6\_4 was also analysed (Figure S25 & S26). Three analyses gave a mean composition of  $78.2\% \pm 2.1\%$  Au,  $14.1\% \pm 1.4\%$  Ag, and  $7.7\% \pm 0.8\%$  Cu, confirming the trace as an Au-alloy.



*Figure S23. DZSWS:STHEAD.6\_1 sampling location (figure produced by C. Tsoraki; photograph taken courtesy of Wiltshire Museum, Devizes).*

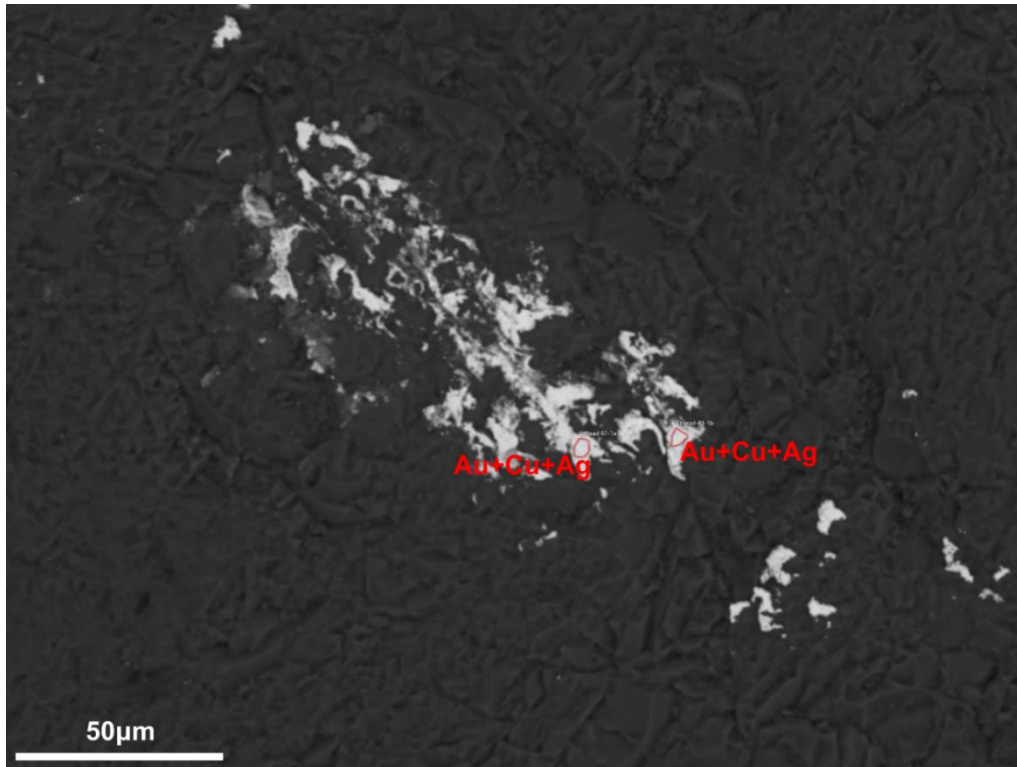


*Figure S24. BSE image of gold-alloy trace (brighter regions) on DZSWS:STHEAD.6\_1. The areas analysed are marked in red (figure produced by C. Standish and R. Pearce).*



*Figure S25. DZSWS:STHEAD.6\_4 sampling location (figure produced by C. Tsoraki; photograph courtesy of Wiltshire Museum, Devizes).*

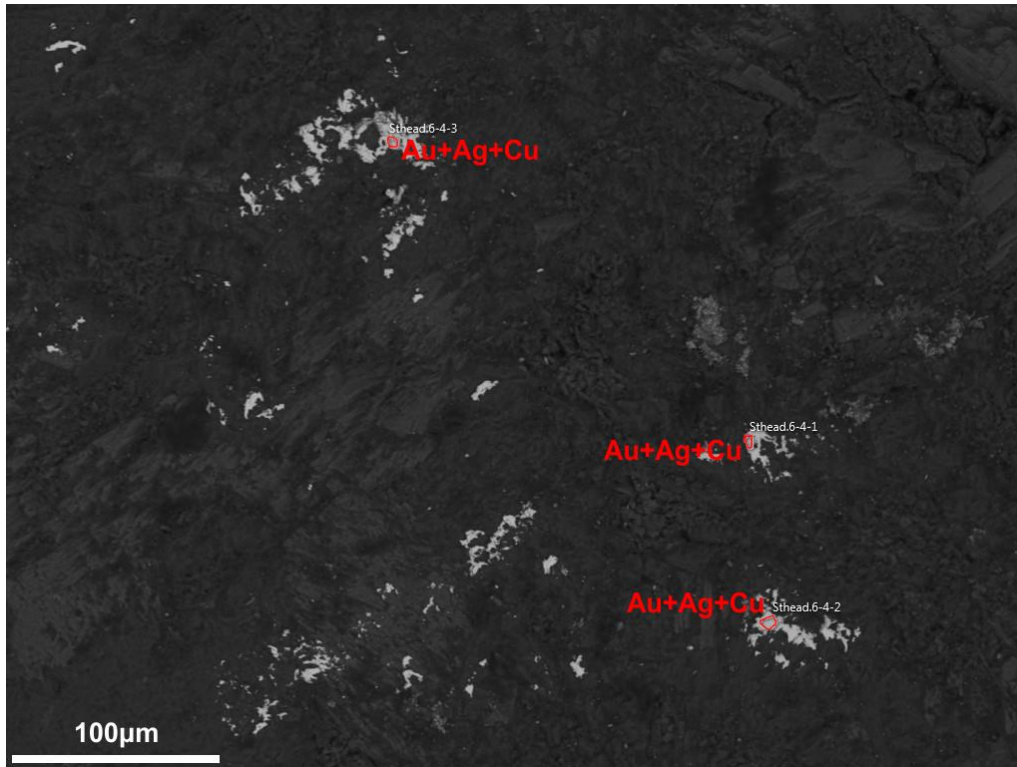


*Figure S26. BSE image of gold-alloy trace (brighter regions) on DZSWS:STHEAD.6\_4. The areas analysed are marked in red (figure produced by C. Standish and R. Pearce).*

Four traces at the same location on the margin of the butt end of battle-axe DZSWS:STHEAD.8 were analysed (Figure S27). One returned the composition of a copper-zinc-tin alloy (56.9% Cu, 41.1% Zn, 2.0% Sn) (Figure S28), whilst the other three indicated the presence of Au-alloy traces (Figure S27–S30). One of these was qualitative only due to the topography of the object partially obscuring the X-ray signal from the SEM detector. The two others gave compositions of 94.6% Au and 5.4% Ag, and 85.8% Au and 14.2% Ag, respectively.



*Figure S27. DZSWS:STHEAD.8 sampling location (figure produced by C. Tsoraki; photograph courtesy of Wiltshire Museum, Devizes).*

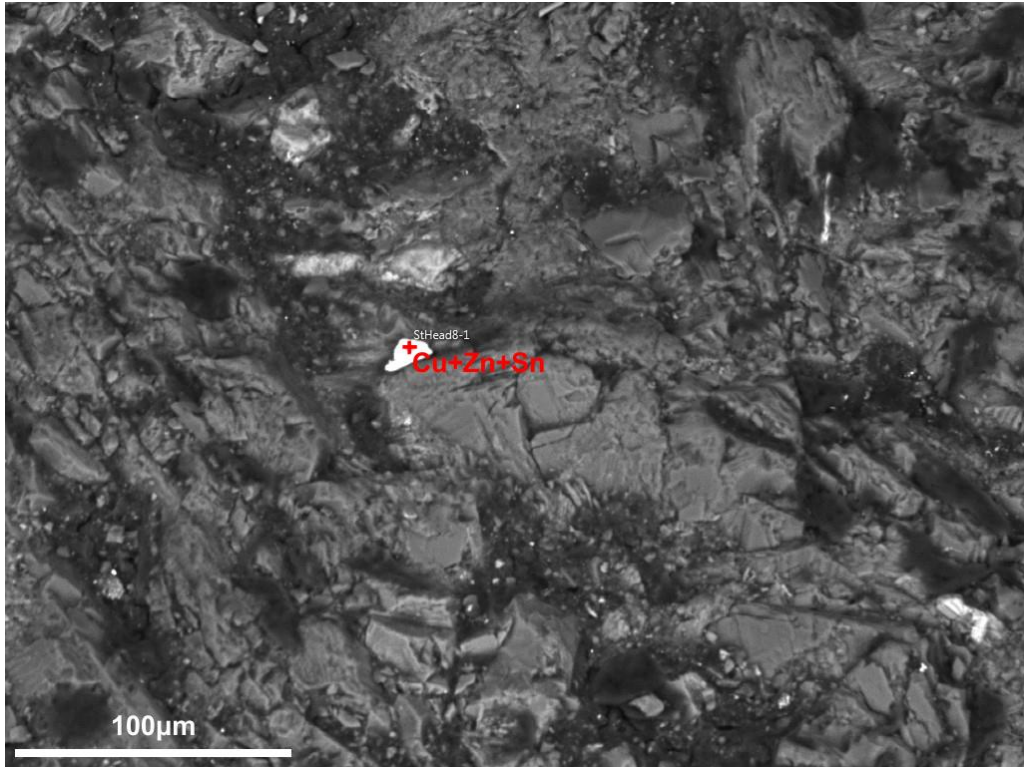


*Figure S28. BSE image of Cu-Zn-Sn trace (brighter area) at location 1 of DZSWS:STHEAD.8. The red cross marks where the compositional analysis was made (figure produced by C. Standish and R. Pearce).*

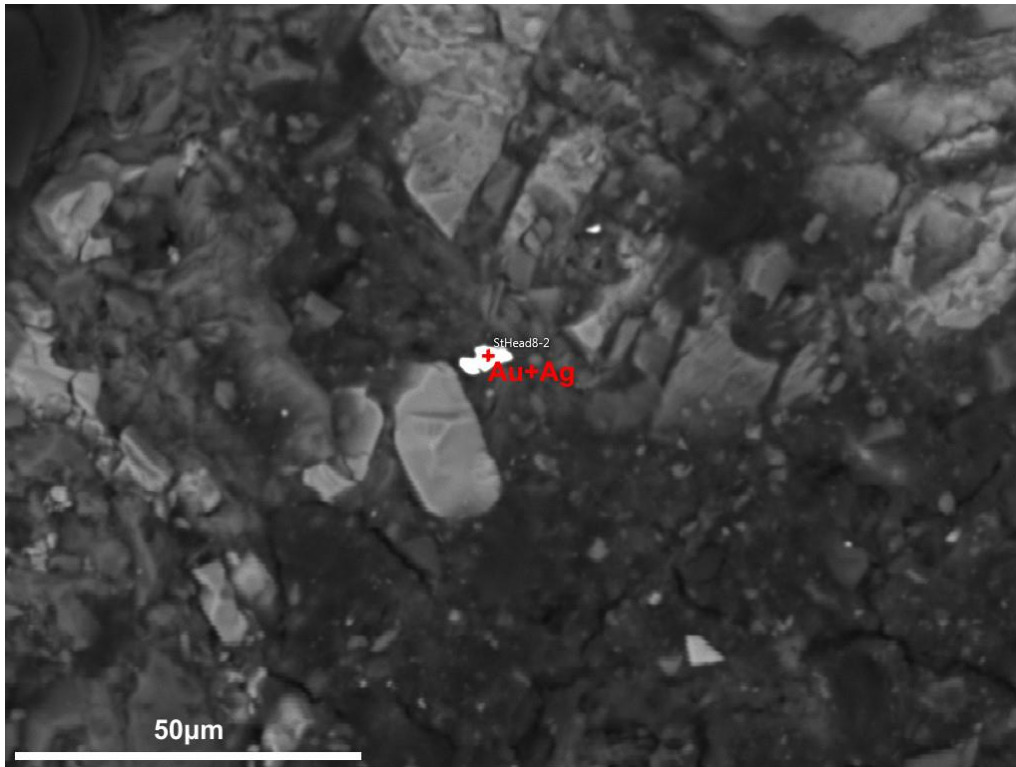


*Figure S29. BSE image of gold-alloy trace, and point of analysis no. 2 (red cross), at sample location 1 of DZSWS:STHEAD.8 (figure produced by C. Standish and R. Pearce).*

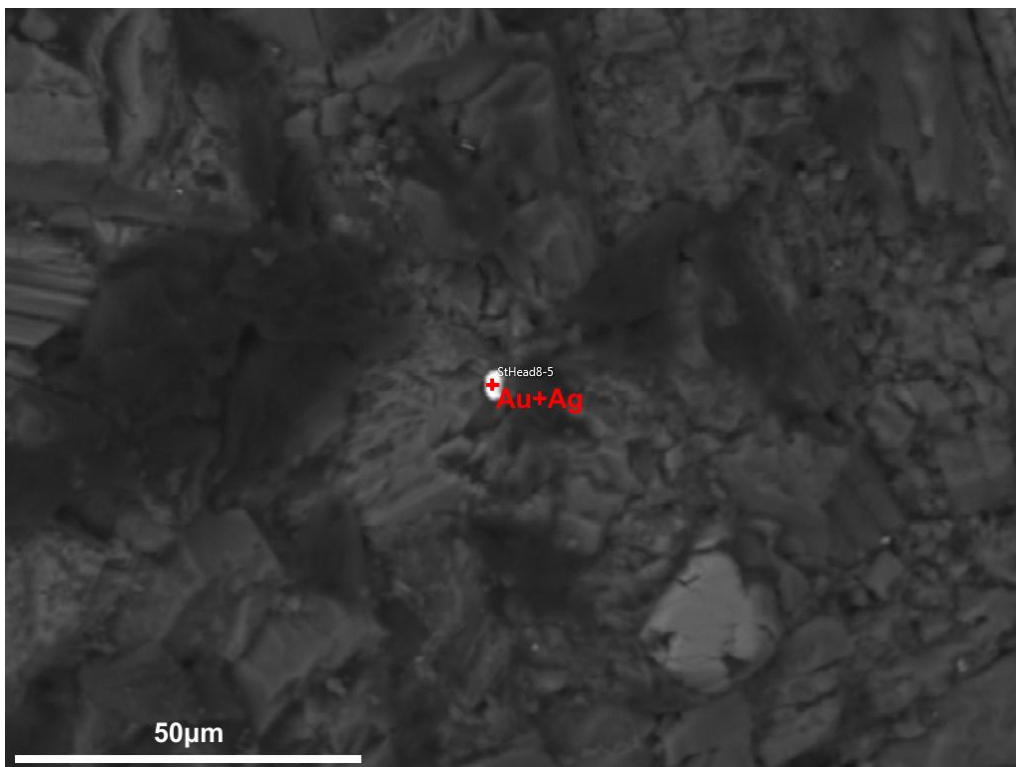


*Figure S30. BSE image of gold-alloy trace, and point of analysis no. 5 (red cross), at sample location 1 of DZSWS:STHEAD.8 (figure produced by C. Standish and R. Pearce).*

Two traces on the cutting edge of flint axe DZSWS:STHEAD.9 were analysed (Figure S31). One was identified as a Au-alloy trace, with a composition of  $93.6\pm 1.5\%$  Au,  $4.2\pm 1.2\%$  Ag, and  $2.2\pm 0.7\%$  Cu (Figure S32). The other was composed of solely of Cu, with no other element identified above the limits of detection (Figure S33).



*Figure S31. DZSWS:STHEAD.9 sampling location (figure produced by C. Tsoraki; photograph courtesy of Wiltshire Museum, Devizes).*

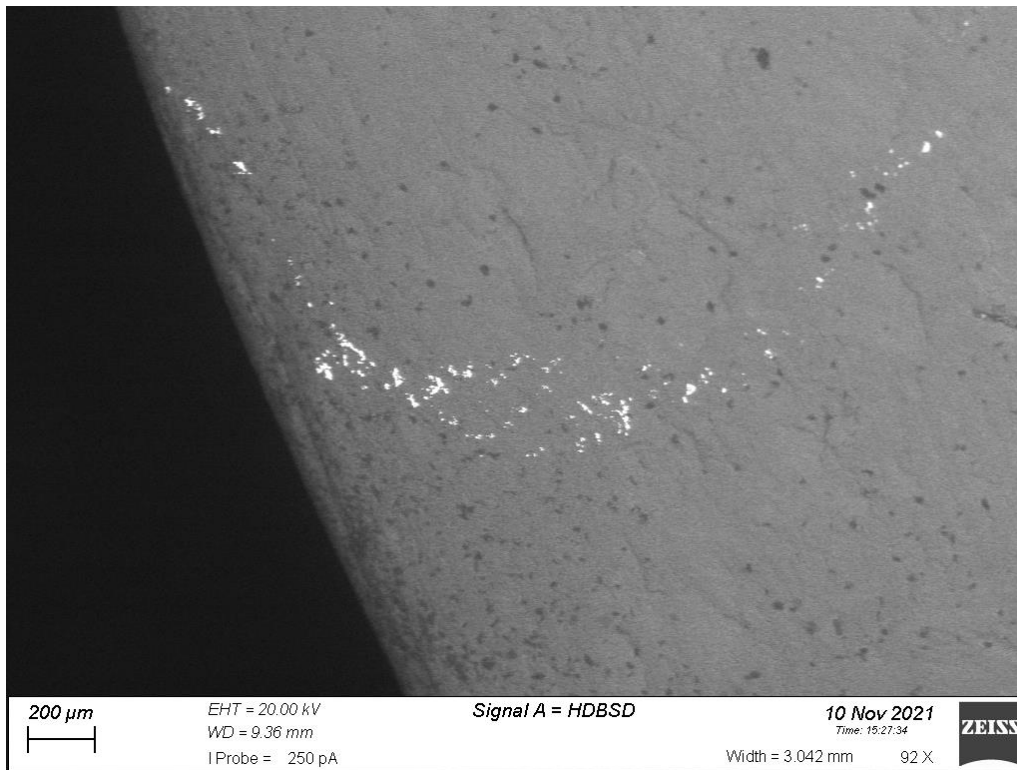


*Figure S32. BSE image of gold-alloy trace (brighter regions) at sample location 1 on DZSWS:STHEAD.9 (figure produced by S. Morriss and C. Standish).*

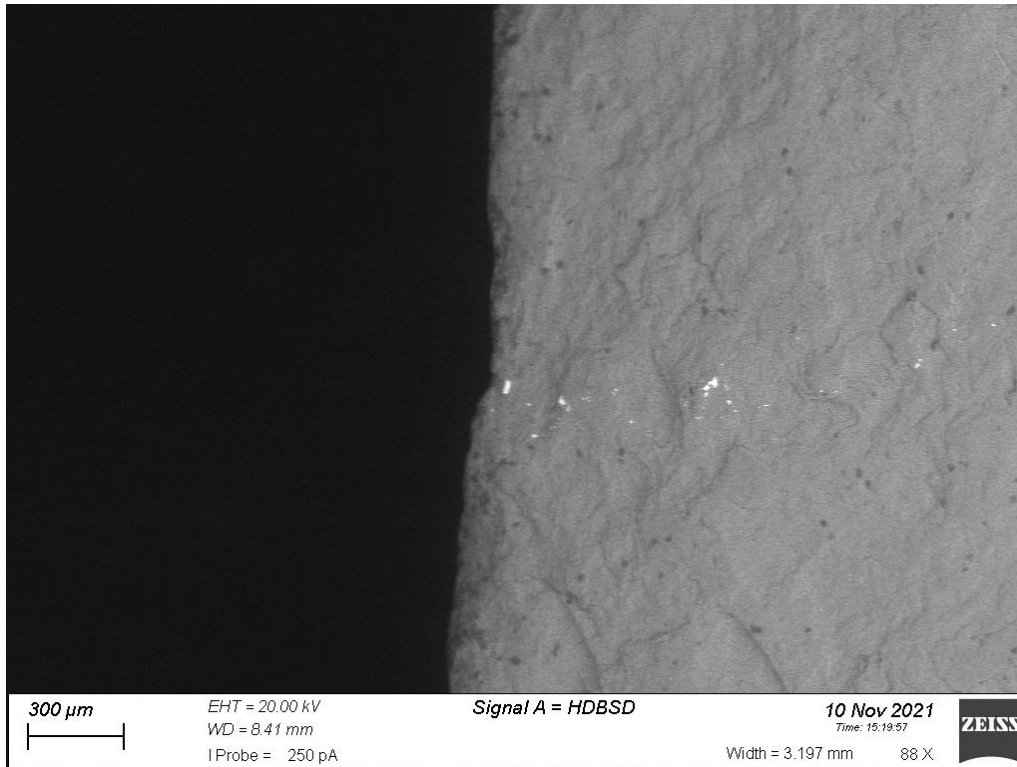


Figure S33. BSE image of copper trace (brighter regions) at sample location 2 on DZSWS:STHEAD.9 (figure produced by S. Morriss and C. Standish).

## Discussion

No gold traces were identified on the copper awl DZSWS:STHEAD.1f. Identified traces on the remaining objects can be divided into four types: 1) gold-alloys (Au-Ag-Cu); 2) copper-alloys; 3) Pb; 4) Fe-Cr-Mn.

### *Au-Alloys*

Six objects have Au-alloy traces, five of which are likely to be ancient. The composition of Chalcolithic and Early Bronze Age (EBA) goldwork from Britain and Ireland ranges from around 70–96% Au, 4–11% Ag, 0–11% Cu, and 0–0.6% Sn with no other elements routinely present on the ~% level (Hartmann 1970, 1982; Standish *et al.* 2015). These ranges are biased by a few objects with quite distinctive or atypical compositions, and it is, for example, more typical for Cu to be present at no more than ~3% or 4% at this time. Looking only at objects from the sheet-gold cover tradition of the EBA—the tradition most relevant to the find contexts of the objects in question—typical compositions in fact range from approximately 76–93% Au, 4–25% Ag, 0–3.5% Cu, and 0–0.5% Sn.

Gold traces were recorded on the polishing stone DZSWS:STHEAD.2a at 6 locations. On Face A, qualitative readings were taken at locations 7 and 8 (Figures S14 & S15). These are in association with Cu-alloy traces; therefore, the composition of both traces cannot be ascertained in any greater detail. Together this suggests the object was used for working both Au and Cu. On Face B, Au-alloy traces were identified at locations 2, 3, 4 and 5 (Figures S9–12). Those taken on the trace at locations 2 and 3 (also analysed by Shell) gave a composition of approximately 85% Au, 13% Ag and 2% Cu. This is consistent with those compositions reported by Shell (2000). The other two traces have compositions that are distinct from those at locations 2 and 3, with approximately 93% Au, 5% Ag and 2.5% Cu. Following comparison to published compositions for EBA goldwork as described above, it is apparent that the Au-alloy traces reported for DZSWS:STHEAD.2a are all consistent with gold alloys typical for the EBA (Figure S34). Moreover, the range in Au-alloy compositions favours the working of a minimum of two, geochemically distinguishable, metal stocks, or ingots/formers, implying that it was used in the production of multiple gold objects.

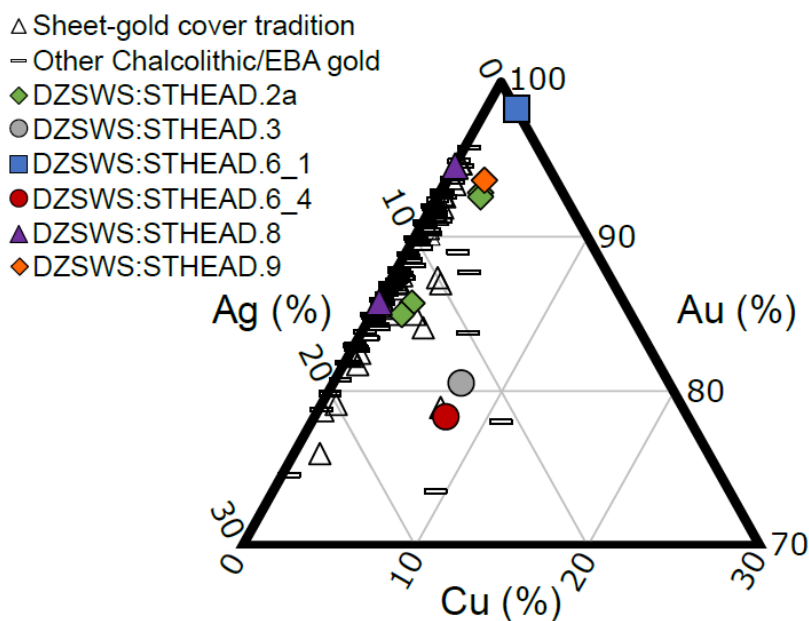


Figure S34. Ternary plot showing alloy compositions (Au-Ag-Cu) of gold-alloy traces recorded on the Upton Lovell G2a stone objects, compared to compositions typical for Chalcolithic and Early Bronze Age goldwork from Britain and Ireland (comparative data from Hartmann 1982 and Standish et al. 2015). Note the gold traces associated with distinct copper traces on DZSWS:STHEAD.2a are not plotted (figure produced by C. Standish).

Object DZSWS:STHEAD.3 has an Au alloy trace, with a recorded composition of approximately 80.5% Au, 12.1% Ag and 7.4% Cu. The Cu content is at the high end of that expected for EBA goldwork and is more typical of Middle and Late Bronze Age goldwork when gold-copper alloying was a common practice. Some high Cu gold alloys do exist in the EBA (Figure S34), however, thus there is no reason to categorically rule out a prehistoric origin (it is also worth noting that this composition is not a clear match to a known, common, modern Au-alloy composition). A similar trace is recorded on object DZSWS:STHEAD.6\_4: 78.2%±2.1% Au, 14.1%±1.4% Ag and 7.7%±0.8% Cu, and could be further evidence of working an Au-alloy with high Cu content. If this was the case, DZSWS:STHEAD.3 and DZSWS:STHEAD.6\_4 were used to work geochemically indistinguishable ingots/formers, and raises the possibility that they may have been used in the manufacturing of the same EBA gold object. An alternate scenario, however, is that this high Cu content may relate to the presence of both Cu and Au traces at the same location on the object, as seen on DZSWS:STHEAD.2a.

Au-alloy traces were recorded at three locations on the cutting edge of the battle-axe DZSWS:STHEAD.8. One is qualitative only, due to the line-of-sight from the SEM detector being partially obscured by the object topography. The other two gave readings of approximately 94.6% Au and 5.4% Ag, and approximately 85.8% Au and 14.2% Ag. An Au-alloy trace was also identified on DZSWS:STHEAD.9 with a composition of approximately 93.6% Au, 4.2% Ag and 2.2% Cu. These traces are within the range of EBA gold alloys and are therefore consistent with the axes being used for prehistoric gold-working. The contrasting compositions of the traces on DZSWS:STHEAD.8 again favour multiple phases of use; that is, it was used to work geochemically distinguishable ingots/formers. It is also of note that these compositions are broadly consistent with the Au-alloy traces identified on DZSWS:STHEAD.2a (where two alloy compositions were identified, one with around 5% Ag and one with around 13% Ag), providing another tangible link between two of the stone objects studied.

Finally, an Au-alloy trace was also identified on DZSWS:STHEAD.6\_1. The analyses gave a relatively pure composition of approximately 98.3% Au, 0.7% Ag and 1.7% Cu. The low Ag makes a prehistoric origin seem somewhat unlikely, raising the possibility of modern origin for the trace. Another possible explanation is that use-wear or post-depositional leaching has altered the composition of the Au-alloy (Scott 1983; Rapson 1996; Troalen *et al.* 2014), with Standish *et al.* (2021) demonstrating that Au-rich zones, spatially focussed on the sample edges and along cracks/fissures within, can be present within Bronze Age artefact gold

alloys. The composition of this trace prevents any further discussion in relation to EBA goldworking.

### *Cu-Alloys*

Cu-alloy traces have been identified on four objects. A Cu-Zn-Sn trace was recorded on the battle-axe DZSWS:STHEAD.8. With Zn at approximately 40%, this is unlikely to be a prehistoric trace, and is more suggestive of contact with a brass implement, either during excavation or post-excavation. A Cu-Zn trace, this time with minor concentrations of Sn, Ag, Al, Fe and Sb, was also identified on the cutting edge portion of battle axe DZSWS:STHEAD.4a\_1. Again, with the high Zn concentration (approximately 24.9–32.0%), this is more suggestive of contact with a metal implement during excavation or post-excavation. A Cu-Sn trace (at a ratio of 3:1) was recorded on DZSWS:STHEAD.2 (grooved abrader), consistent with bronze working in prehistory. Two traces on polishing stone DZSWS:STHEAD.2a recorded high levels (>20%) of Cu alongside Au. These are distinguishable from the Au on the SEM images (e.g. Figure S15), and therefore rather than representing a high Cu gold alloy, working of both Cu-alloys and Au-alloys in prehistory is a more likely scenario. Traces of Cu+Sn were noted on anvil DZSWS:STHEAD.6\_1, whilst a Cu trace was identified on DZSWS:STHEAD.9, suggesting that these objects may also have been used for working both Cu- and Au-alloys (see discussion above).

### *Pb*

Three objects recorded Pb signals: DZSWS:STHEAD.2, DZSWS:STHEAD.2a, and DZSWS:STHEAD.3, with Pb also noted on a fourth (DZSWS:STHEAD.6\_1). No other elements were recorded above the limit of detection alongside, except for those present in the matrix of the rock. The origin of the Pb is unclear: the signals could be associated with Pb-based minerals within the rock, with post-excavation processes, or from processing materials containing Pb in prehistory.

### *Fe-Cr-Mn*

A Fe-Cr-Mn trace was identified on the butt-end of battle axe DZSWS:STHEAD.4a\_2, which most likely represents contact with a steel implement during either excavation or post-excavation. This is consistent with apparent post-excavation traces on the other portion of this object, DZSWS:STHEAD.4a\_1.



**Table S1. Concordance table detailing the terminology used by previous authors to describe the various grave goods from Upton Lovell.**

<b>Grave goods</b>	<b>Piggott 1962</b>	<b>Annable &amp; Simpson (1964: 49–50, drawings 104)</b>	<b>Woodward &amp; Hunter (2015)</b>
Perforated bone points	41 perforated bones points	41 Perforated bone points	44 bone points; Class 2; many made from lower rear sheep legs (p97–109)
Unperforated bone points	2 bone pendants	2 unperforated bone points	Potentially incorporated within the perforated bone group
Awl	Not mentioned	Bronze awl	Copper alloy awl; Group 2A/B (p89–96)
Flint axes	4 Flint axes	Flint axes	No
Grooved stone	Grooved shaft-smoother	Grooved whetstone	Grooved stone (p73–75)
Modified stone cobbles	9 stone rubbers or polishers	9 stone rubbers	No
Polished parallelepiped objects (reworked battle axes)	9 stone rubbers or polishers	9 stone rubbers	No
Polished stone	9 stone rubbers or polishers	9 stone rubbers	No
Stone slab	9 stone rubbers or polishers	9 stone rubbers	No
Two fragments of battle axe	Fragments of a broken battle axe	Broken battle axe	No
Flint nodule cups	4 marcasite 'cups'	Aetites or eagle stones	No
Complete battle axe	Dolerite shaft hole battle axe	Complete axe from Group XVIII	No
Jet belt ring	Jet ring	Shale ring	Jet belt ring; Class 1; worn, possible heirloom (p59–60)
Jet bead	Not mentioned	Shale beads	3 jet-like beads (p425–27)
Bone bead	Not mentioned	Bone Bead	Bone bead; distal shaft sheep tibia

			(p425–27)
Three boars' tusks	Boar's tusk pendants	Boar's tusks; one perforated two damaged at broad end	Perforated boar's tusks (p141–45)

**Table S2. Summary data regarding the production and making of different sheet gold items discussed in research by Woodward and Hunter (2015) and associated papers. IL&D = incised lines and dots; IL = incised lines; ID = incised dots; R&F = rib and furrow.**

Site	Object	Style of decoration	Size of incision (mm)	Suggested tool(s) for decoration and application	Perforations (size in mm, where given)	Composite materials ( <b>bold</b> indicates identification; <i>italics</i> indicates suggestion)	Source (Woodward & Hunter (2015) unless stated)
Clandon, Dorset	Jet macehead with gold-covered shale studs	None	NA	Burnisher to fit the gold to the stud	One perforation jet macehead	<b>jet macehead; Kimmeragh shale studs</b> ; <i>adhesive</i>	Needham & Woodward 2008: 22–27
Clandon, Dorset	Gold lozenge plaque	IL&D	0.33 average	U-shaped profile, narrow, but not sharp	One but likely post-depositional	<i>wood core; resin</i>	Needham & Woodward 2008: 13–22
Little Cressingham, Norfolk	Goldsheet rectangular plaque	IL&D	0.5–1	Very fine but blunt tool; possibly bone or wood	Six perforations (1.2)	<i>wood or other perishable material</i>	p 213–16
Little Cressingham, Norfolk	Three goldsheet cap ends	R&F	NA	–	No	<i>traces of adhesive residue within the cap</i>	p 216–19
Little Cressingham, Norfolk	Goldsheet corrugated band	R&F	NA	Tool to apply light pressure to shape	No	NA	p 219–20
Manton barrow,	Halberd pendant	IL	0.25	–	Two perforations (0.5; 4.0)	<b>amber shaft; copper alloy blade; copper/alloy rivets</b>	p 194; 231–32

Preschute G1a, Wiltshire							
Manton barrow, Preschute G1a, Wiltshire	Lignite and gold bead	IL	Not given	–	Lignite bead perforation (5.7)	<b>Lignite/shale</b>	p 448–50
Manton barrow, Preschute G1a, Wiltshire	Gold bound amber disc	IL&D	Not given	–	One V- perforation	<b>amber</b>	p 448–50
Mere G6a, Wiltshire	Goldsheet disc	IL&D	<1	Flint blade or sharp bone edge	Two perforations (1.0)	<i>stitched to a garment; unknown core</i>	p 209–10
Ridgeway 7, Weymouth G8, Dorset	Gold sheet pommel cover	IL	Not given	–	–	<i>wood</i>	p 46–47
Upton Lovell G2e, Wiltshire	Goldsheet rectangular plaque	IL	0.2–3 lines; 0.1–2 lattice	Two tools: thicker V-section tool; finer rounded-end tool for lattice (possibly a comb)	Four perforations (1.7–2)	<i>wood or other perishable material</i>	p 220–22
Upton Lovell G2e, Wiltshire	4 goldsheet cap end	R&F	None	–	Possible, but not clear if ancient or modern	unknown	p 225–27

Upton Lovell G2e, Wiltshire	11 goldsheet covered beads	ID	0.5	–	Two per item, (0.8–1.7)	light grey material	p 227–29
Upton Lovell G2e, Wiltshire	Conical pendant or button	IL	0.1–0.3	2 tools: U-shaped profile tool and a lighter, thinner tool	One perforation (1.5×3 oblong)	<b>shale or jet</b>	p 222–25
Wilsford G5, Bush Barrow, Wiltshire	Gold sheet lozenge plaque	IL	0.7	Sub-V-shaped profile	Two perforations (1–1.3)	<i>wood</i>	p 236–38
Wilsford G5, Bush Barrow, Wiltshire	Goldsheet belt hook cover	IL	Not given	Sub-V-shaped profile	Five perforations (0.5)	<i>wood</i>	p 238–42
Wilsford G5, Bush Barrow, Wiltshire	Goldsheet lozenge plaque	IL	0.25	V shaped profile	none	unknown	p 235–37
Wilsford G7, Wiltshire	Gold covered shale sphere	IL	1	–	Two V- perforations	<b>shale</b>	p 194–97; 450–51
Wilsford G7, Wiltshire	Gold pendant	IL	Not given	–	V-perforation	not given	p 194–97; 442–43
Wilsford G8, Wiltshire	Conical pendant	IL&D	0.1	–	1.7×1.2mm and 1.7×1.6mm	<b>shale</b>	p 229–31
Wilsford G8, Wiltshire	Halberd pendant	IL	Not given	–	Amber shaft has a 1.5mm perforation	<b>amber shaft; copper alloy blade; copper/alloy rivets</b>	p 230–33; 194

Wilsford G8, Wiltshire	Goldsheet covered penannular pendant	ID	Not given	–	none	<b>copper</b>	p 194–97; 450–51
Wilsford G8, Wiltshire	Goldsheet covered bone pendant	IL	0.5–0.9	–	2 × 0.9mm	<b>mammal bone</b>	p 194–97; 450–51
Wilsford G8, Wiltshire	2 gold bound amber discs	IL&D	Not given	–	V-perforation	<b>amber</b>	p 194–96; 442–43
Wilsford- Cum-Lake G47, 49 or 50	2 goldsheet domed button covers	Lines - possibly lightly pressed rather than truly incised	0.4–0.7	Three tools of different width points: 0.7mm; 1.2mm; 2mm	No	unknown	p 212–13
Wilsford- Cum-Lake G47, 49 or 50	2 goldsheet discs	ID	Not given	–	No	<i>Wood; leather; adhesive</i>	p 210–12

## References

- ADAMS, J.L. 2002. *Ground stone analysis: a technological approach*. Salt Lake City: University of Utah Press.
- ADAMS, J. *et al.* 2009. Functional analysis of macro-lithic artefacts: a focus on working surfaces, in F. Sternke, L. Eigeland & L. J. Costa (ed.) *Non-flint Raw material use in prehistory: old prejudices and new directions* (British Archaeological Reports International Series 1939): 43–66. Oxford: Archaeopress.
- ANNABLE, F.K. & D.D.A. SIMPSON. 1964. *Guide catalogue of the Neolithic and Bronze Age collections in Devizes Museum*. Devizes: Wiltshire Archaeological and Natural Historical Society.
- BOUTOILLE, L. 2019. Cushion stones and company: British and Irish finds of stone metalworking implements from the Bell Beaker period to the Late Bronze Age, in D. Brandherm (ed.) *Aspects of the Bronze Age in the Atlantic archipelago and beyond. Proceedings from the Belfast Bronze Age Forum 9–10 November 2013* (Archaeologia Atlantica Monographiae III): 203–17. Hagen/Westfalen: Curach bhán.
- CARICOLA, I. *et al.* 2020. Prehistoric exploitation of minerals resources: experimentation and use-wear analysis of grooved stone tools from Grotta della Monaca (Calabria, Italy). *Archaeological and Anthropological Sciences* 12: 259. <https://doi.org/10.1007/s12520-020-01219-7>
- DELGADO-RAACK, S. 2008. Prácticas económicas y gestión social de recursos (macro)líticos en la prehistoria reciente (III–I milenios ac) del mediterráneo occidental. Unpublished PhD dissertation, Universitat Autònoma de Barcelona. Available at: <http://hdl.handle.net/10803/5528> (accessed 11 November 2022).
- DELGADO-RAACK, S. & R. RISCH. 2008. Lithic perspectives on metallurgy: an example from Copper and Bronze Age south-east Iberia, in L. Longo & N. Skakun (ed.) “*Prehistoric technology*” 40 years later: functional studies and the Russian legacy. *Proceedings of the international congress (Verona 2005)* (British Archaeological Reports International series 1783): 235–51. Oxford: Archaeopress.
- DUBREUIL, L. *et al.* 2015. Current analytical frameworks for studies of use-wear on ground stone tools, in J. Manuel Marreiros, J.F. Gibaja Bao & N. Ferreira Bicho (ed.) *Use-wear and residue analysis in archaeology*: 105–58. Springer: New York.
- EVENS, E. D., L.V. GRINSELL, S. PIGGOTT & F.S. WALLIS. 1962. Fourth report of the sub-committee of the south-western group of museums and art galleries on the petrological

- identification of stone axes. *Proceeding of the Prehistoric Society* 28: 209–66.  
<https://doi.org/10.1017/S0079497X00015723>
- EVENS, E. D., I.F. SMITH & F.S. WALLIS. 1972. The petrological identification of stone implements from south-western England: fifth report of the sub-committee of the south-western federation of museums and art galleries. *Proceeding of the Prehistoric Society* 38: 235–75. <https://doi.org/10.1017/S0079497X00012135>
- VAN GIJN, A.L. 2010. *Flint in focus: lithic biographies in the Neolithic and Bronze Age*. Leiden: Sidestone.
- 2014. Science and interpretation in microwear studies. *Journal of Archaeological Science* 48: 166–69. <https://doi.org/10.1016/j.jas.2013.10.024>
- VAN GIJN, A.L. & R. HOUKES 2006. Stone, procurement and use, in L.P Louwe Kooijmans & P Jongste (ed.) *Schipluiden: a Neolithic settlement on the Dutch North Sea coast c. 3500 cal BC* (Analecta Prehistorica Leidensia 37/38): 167–94. Leiden: Faculty of Archaeology.
- HAMON, C. 2008. Functional analysis of stone grinding and polishing tools from the earliest Neolithic of north-western Europe. *Journal of Archaeological Science* 35: 1502–20.  
<https://doi.org/10.1016/j.jas.2007.10.017>
- HAMON, C. *et al.* 2020. Tracking the first bronze metallurgists of Western Europe: combined use-wear analysis and X-ray fluorescence synchrotron spectroscopy of a stone toolkit from Ploneour-Lanvern (Brittany). *Archaeological and Anthropological Sciences* 12: 14.  
<https://doi.org/10.1007/s12520-019-00999-x>
- HARTMANN, A. 1970. *Prähistorische Goldfunde aus Europa: Spektralanalytische Untersuchungen und deren Auswertung*. Berlin: Gebr. Mann.
- 1982. *Prähistorische Goldfunde aus Europa II: Spektralanalytische Untersuchungen und deren Auswertung*. Berlin: Gebr. Mann.
- HAYES, E., C. PARDOE & R. FULLAGAR. 2018. Sandstone grinding/pounding tools: use-trace reference libraries and Australian archaeological applications. *Journal of Archaeological Science Reports* 20: 97–114. <https://doi.org/10.1016/j.jasrep.2018.04.021>
- LI, W. *et al.* 2018. New insights into the grinding tools used by the earliest farmers in the central plain of China. *Quaternary International* 529: 10–17.  
<https://doi.org/10.1016/j.quaint.2018.10.005>
- MOORE, D.T. & W.A. ODDY. 1985. Touchstones: some aspects of their nomenclature, petrography and provenance. *Journal of Archaeological Science* 12: 59–80.  
[https://doi.org/10.1016/0305-4403\(85\)90015-9](https://doi.org/10.1016/0305-4403(85)90015-9)

- NEEDHAM, S. & A. WOODWARD. 2008. The Clendon barrow finery: a synopsis of success in an Early Bronze Age world. *Proceedings of the Prehistoric Society* 74: 1–52.  
<https://doi.org/10.1017/S0079497X00000128>
- PIGGOTT, S. 1962. From Salisbury Plain to Siberia. *Wiltshire Archaeological and Natural History Magazine* 58: 93–97
- RAPSON, W.S. 1996. Tarnish resistance, corrosion and stress: corrosion cracking of gold alloys. *Gold Bulletin* 29: 61–69. <https://doi.org/10.1007/BF03215466>
- ROE, F.E.S. 1966. The battle-axe series in Britain. *Proceeding of the Prehistoric Society* 32: 199–245. <https://doi.org/10.1017/S0079497X00014390>
- 1979. Typology of stone implements with shaftholes, in T.H.M. Clough & W.A. Cummins (ed.) *Stone axe studies: archaeological, petrological, experimental, and ethnographic* (Council for British Archaeology Research Report 23): 23–48. London: Council for British Archaeology.
- SCOTT, D.A. 1983. The deterioration of gold alloys and some aspects of their conservation. *Studies in Conservation* 28: 194–203. <https://doi.org/10.2307/1505967>
- STANDISH, C.D., B. DHUIME, C.J. HAWKESWORTH & A.G.W. PIKE. 2015. A nonlocal source of Irish Chalcolithic and Early Bronze Age gold. *Proceedings of the Prehistoric Society* 81: 149–77. <https://doi.org/10.1017/ppr.2015.4>
- STANDISH, C.D. *et al.* 2021. Archaeological applications of natural gold analyses, in T. Torvela, J.S. Lambert-Smith & R.J. Chapman (ed.) *Recent advances in understanding gold deposits: from orogeny to alluvium* (Geological Society, London, Special Publications 516). Early View. <https://doi.org/10.1144/SP516-2021-59>
- TROALEN, L.G., J. TATE & M.F. GUERRA. 2014. Goldwork in ancient Egypt: workshop practices at Qurneh in the 2<sup>nd</sup> Intermediate period. *Journal of Archaeological Science* 50: 219–26. <http://doi.org/10.1016/j.jas.2014.07.010>
- TSORAKI, C. 2008. Neolithic society in northern Greece: the evidence of ground stone artefacts. Unpublished PhD dissertation, University of Sheffield.
- 2012. Ground stone technologies at the Bronze Age settlement of Sissi: preliminary results, in J. Driessen *et al.* (ed.) *Excavations at Sissi III. Preliminary report on the 2011 campaign*: 201–21. Louvain-la-Neuve: Presses Universitaires de Louvain.
- 2021. The ground stone technologies at Neolithic Çatalhöyük: issues of production, use and deposition, in I. Hodder (ed.) *Materials at Çatalhöyük: reports from the 2009–2017 seasons* (Çatalhöyük Research Project Series Volume 14): 309–70. London: British Institute at Ankara.

- TSORAKI, C., H. BARTON, R.J. CRELLIN & O.J.T. HARRIS. 2020. Making marks meaningful: new materialism, microwear and the world of material signs. *World Archaeology* 52: 484–502. <https://doi.org/10.1080/00438243.2021.1898462>
- VERBASS, A. & A.L. VAN GIJN. 2007. Querns and other hard stone tools from Geleen-Janskamperveld, in P. van de Velde (ed.) *Excavations at Geleen-Janskamperveld 1990/1991* (Analecta Praehistorica Leidensia 39): 191–204. Leiden: Faculty of Archaeology.
- WILLIAMS-THORPE, O., P.C. WEBB & M.C. JONES. 2003. Non-destructive geochemical and magnetic characterisation of Group XVIII dolerite stone axes and shaft-hole implements from England. *Journal of Archaeological Science* 30: 1237–67. [https://doi.org/10.1016/S0305-4403\(02\)00274-1](https://doi.org/10.1016/S0305-4403(02)00274-1)
- WOODWARD, A. & J. HUNTER (ed.). 2015. *Ritual in Early Bronze Age grave goods: an examination of ritual and dress equipment from Chalcolithic and Early Bronze Age graves in England*. Oxford: Oxbow.
- WOODWARD, A. & S. NEEDHAM. 2012. Diversity and distinction: characterising the individual buried at Wilsford G58, Wiltshire, in A.M. Jones, J. Pollard, M.J. Allen & J. Gardiner (ed.) *Image, memory and monumentality: archaeological engagements with the material world*: 116–26. Oxford: Oxbow. <https://doi.org/10.2307/j.ctvh1dhcs.24>